Molina Puerto, J.; Fernández Sáez, J.; Fernandes, M. ; Souto, A.P.; Esteves, M.F.; Bonastre Cano, JA.; Cases, F. (2015). Plasma treatment of polyester fabrics to increase the adhesion of reduced
graphene oxide. Synthetic Metals. 202:110-122. doi:10.1016/j.synthmet.2015.01.023.

Plasma treatment of polyester fabrics to increase the adhesion of reduced graphene oxide

J. Molina,[1,2] J. Fernández,[1] M. Fernandes,[2] A.P. Souto,[2] M.F. Esteves,[2] J. Bonastre,[1] F. Cases[1]*

[1]*Departamento de Ingeniería Textil y Papelera, EPS de Alcoy, Universitat Politècnica de València, Plaza Ferrándiz y Carbonell s/n, 03801 Alcoy, Spain*

[2]*Department of Textile Engineering, University of Minho, Campus de Azurém, 4800-058 Guimarães, Portugal*

Abstract

Polyester (PES) fabrics were treated with plasma to enhance the adhesion of reduced graphene oxide (RGO) and produce conductive fabrics. The surface energy of the plasma treated fabrics was measured using contact angle measurements and showed a stabilization of this parameter with plasma dosages of 3000 $W \cdot min \cdot m^{-2}$. The surface roughness measured by atomic force microscopy (AFM) also showed a stabilization with the same plasma dosage value. The plasma treatment induced negative charges on the surface of the fibers and graphene oxide (GO) also presented negative charges – and so deposition of GO on the surface of the PES fibers was not possible. For this reason, bovine serum albumin (BSA) was employed as an intermediate coating that acquired a positive charge and enabled the self-assembly of GO on plasma treated PES fibers. Electrochemical impedance spectroscopy (EIS) was employed to measure the resistance of the conductive fabrics. The plasma treatment and BSA coating improved the coating level of the samples and hence the conductivity of the fabrics was improved with the

application of fewer RGO layers. RGO adhesion on fabrics was also improved as shown in rubbing fastness tests.

Keywords: dielectric barrier discharge (DBD), adhesion, polyester, reduced graphene oxide, conductive fabrics.

---

* Corresponding author. Fax.: +34 966528438; telephone: +34 966528412.

E-mail addresses: jamopue@doctor.upv.es (J. Molina), jaferse1@posgrado.upv.es (J. Fernández), marta.fernandes@det.uminho.pt (M. Fernandes), souto@det.uminho.pt (A.P. Souto), festeves@det.uminho.pt (M.F. Esteves), joboca@txp.upv.es (J. Bonastre), fjcases@txp.upv.es (F. Cases).

1. Introduction

In the field of textiles there is increasing interest in the development of fabrics with new properties such as: flame resistance [1]; self-cleaning [2]; thermal regulation [3]; electrical conduction [4]; or even catalysis [5]. Among these properties, electrical conductivity has attracted particular attention. Conductive fabrics can be employed for the production of smart textiles with the integration of sensors or various electronic devices [6, 7]. Various approaches can be used to produce conductive fabrics. For instance, the use of metallic fibers inserted in the fabric has been reported; however, the continuous bending and stretching that take place in fabrics produce breakages in the fibers [4]. This is why other approaches have been investigated: the extrusion of fibers with conductive particles such as carbon derivatives [8], or the synthesis of conducting polymer films on the fabrics [9-11].

The discovery of graphene and its derivatives has opened a new era in the field of physics and materials science [12]. The outstanding optical, electronic, thermal and mechanical properties shown by this material have created expectations regarding various possible applications [12-19]. Different methods have been employed for the production of graphene and its derivatives [18-20]. Mechanical exfoliation of graphite crystals was the first method reported by Novoselov *et al. [*12]. Although the quality of graphene produced in this way is excellent; the quantity of graphene that can be obtained is minimal and can only be used for fundamental studies. This is why other methods such as chemical vapor deposition or chemical methods have been continuously developed in response to the increasing demand for graphene materials. Chemical methods have been proposed as a cheaper alternative and with higher production capacity than chemical vapor deposition. One of these methods is the production of graphene oxide (GO) by the oxidation of graphite. The oxidation of graphite allows the exfoliation of graphene oxide layers. However, a reduction step is necessary to convert the insulating GO into conducting reduced graphene oxide (RGO) [20].

Regarding the application of graphene and derivatives to produce conductive fabrics, the most widely employed method has been the adsorption of GO on the fabric or fibers and its posterior reduction to produce RGO [21-28]. Graphene oxide sheets are adsorbed on the surface of the fabrics due to the attraction forces between the oxidized groups of GO and the functional groups of the fabrics. The direct deposition of graphene on fabrics has also been reported by Yu *et al*. [29]. In the present paper the adsorption/reduction strategy has been employed to produce RGO coated polyester fabrics. Plasma techniques have been widely used to increase the adhesion between different materials, including polymers [30]. Plasma treatment produces reactive groups

and radicals on the surface of treated fabrics. In the case of polyester, plasma treatment can oxidize the polyester surface by breaking the ester bonds and creating radicals [31]. These radicals are able to react with the plasma gas generated and create hydroxyl, carbonyl, and carboxyl groups. These polar groups form dipolar interactions, van der Waals forces or hydrogen bonds between the fabric and the coating, thereby increasing the adhesion of the coating to the surface of the fabric [30, 32]. In addition to the creation of functional groups, an increase in roughness on the surface of the fabrics takes place due to the removal of material. The rougher surface allows a better contact between the fibers and the coating and enhances its adhesion [30, 31]. The novelty of the paper is the increase in the adhesion of RGO sheets to the surface of the fabrics after applying a plasma technique. The plasma treatment was combined with a bovine serum albumin (BSA) intermediate layer that converted the negative charges generated by plasma treatment on the fabric surface into positive charges, this allowed self-assembly with GO sheets that possess a negative charge before the reduction to RGO. The effect of this treatment on the electrical resistance of the modified fabrics will also be explored.

There are various plasma methods available. In the present work we have used dielectric barrier discharge (DBD). This technique is a type of cold plasma generated by an electric discharge in atmospheric conditions. Electrical discharge takes place between two electrodes separated by a small gap where the fabric is continuously treated at a controlled speed. Fabric modification by plasma methods has the advantage that no water or other chemical products are needed. The low temperature produced by DBD also allows little deterioration of organic samples [33].

2. Experimental

2.1. Reagents and materials

All the reagents used were of analytical grade.

For the synthesis: monolayer graphene oxide (GO) powders were acquired from Nanoinnova Technologies SL (Spain); sodium dithionite ($Na_2S_2O_4$) was acquired from Merck; and bovine serum albumin (BSA) was acquired from Sigma Aldrich. The polyester fabric characteristics were: fabric surface density, 100 $g \cdot m^{-2}$; warp threads per cm, 55; weft threads per cm, 29. These are specific terms used in the textile industry and their meaning can be consulted in a textile glossary [34].

For the characterization: sulphuric acid (H_2SO_4) and potassium chloride (KCl) were purchased from Merck. $K_3Fe(CN)_6$ 99% was used as received from Acrōs Organics.

When needed, solutions were deoxygenated by bubbling nitrogen (N_2 premier X50S). Ultrapure water was obtained from an Elix 3 Millipore-Milli-Q Advantage A10 system with a resistivity of nearly 18.2 $M\Omega \cdot cm$.

2.2. Dielectric barrier discharge (DBD) treatment

Plasma treatment of polyester was carried out at atmospheric pressure with the dielectric barrier discharge modality (DBD) (Softal/University of Minho patented prototype) [35]. The laboratorial prototype machine used in this work has a width of 50 cm and consisted of the following components: a metallic electrode coated with ceramic; a metallic counter electrode coated with silicone; an electric generator and a high tension transformer. The velocity (v) and power (P) are variable and the fabric passed through the electrodes continuously. The plasma dosage was defined by the equation (1) [35]:

$$dosage = \frac{N \cdot P}{v \cdot w} \qquad (1)$$

Where: N (number of passages); P (power, W); v (velocity, $m \cdot min^{-1}$); and w (width, 0.5 m). For the treatment of polyester fabrics, velocity and power were maintained constant and the number of passages was varied. Table 1 shows the conditions created for the treatments. ~~The laboratorial prototype machine used in this work has a width of 50 cm so fabrics up to this width can be treated; several meters of fabric can be treated at a time.~~

2.3. Contact angle measurements

For measuring the contact angles of the water drops in untreated and plasma treated polyester fabrics we used Goniometer Dataphysics equipment and OCA software with a video system for the caption of images in static and dynamic modes. A drop of 5 µl of distilled water was placed on the fabric surface with a microliter syringe and observed with a special CCD camera. At least ten measurements at different places were taken for each fabric. The camera takes an image every 0.04 sec.

To calculate the surface energy (γ) and its polar (γ^P) and dispersive components (γ^D) the Wu method (harmonic-mean) was used [36]. The surface energy (γ) is considered to be composed of polar and dispersive components. In particular, the polar component results from three different intermolecular forces due to permanent and induced dipoles and hydrogen bonding, whereas the dispersion (non-polar) component is due to instantaneous dipole moments. For polar solids or liquids, the total γ is a sum of the always-existing London dispersion forces (γ^D) with intermolecular interactions that depend on the chemical nature of the material, compiled as polar forces (γ^P):

$$\gamma = \gamma^D + \gamma^P \quad (2)$$

The polar and dispersive components of the surface energy (γ^D and γ^P, respectively) were calculated using the Wu method (harmonic mean) in equation 3:

$$\gamma_{sl} = \gamma_s + \gamma_l - 4\left[\frac{\gamma_s^D \gamma_l^D}{\gamma_s^D + \gamma_l^D} + \frac{\gamma_s^P \gamma_l^P}{\gamma_s^P + \gamma_l^P}\right] (3)$$

Three liquids with known surface energy and surface energy components were used in this study to calculate the surface energy components of the fabrics: distilled water (γ: 72.8; γ^D: 29.1; γ^P: 43.7); polyethylene glycol 200 (PEG) (γ: 43.5; γ^D: 29.9; γ^P: 13.6); and glycerol (γ: 63.4; γ^D: 37.4; γ^P: 26.0). The units used are $mJ \cdot m^{-2}$.

2.4. Synthesis of reduced graphene oxide on polyester fabrics

Polyester fabrics were coated with reduced graphene oxide (RGO) similar to Fugetsu *et al.* [26]. A 3 g L^{-1} GO solution was obtained sonicating GO monolayer powders in an ultrasound bath for 60 min. The first stage of the synthesis was carried out by putting the GO solution in contact with the fabric to allow the adsorption of GO sheets on the surface of the fabrics. This stage lasted 60 minutes. The fabrics with GO were then dried for 24 h under ambient conditions. The second stage of the synthesis was the reduction of GO to RGO. Fabrics coated with GO were placed for 30 min in a solution containing the reducer (50 mM $Na_2S_2O_4$) at approximately 90º C. Samples with a different number of RGO coatings (1 to 10) were obtained (PES-1G to PES-10G) repeating the procedure mentioned above. The samples treated with plasma were also coated with RGO following the same procedure. The plasma treatment generates negative charges on the surface of the fabrics, GO also presents negative charges so the deposition of GO on the fabrics is not possible under these conditions. For this reason, bovine serum albumin (BSA) was employed as an intermediate coating as it acquires a positive charge and allows the deposition of GO on the surface of the fabrics. A 0.5 % weight aqueous BSA solution [25] prepared at room temperature was employed to coat the plasma treated PES samples. Fabrics were placed in contact with the solution at

room temperature for 15 minutes with magnetic stirring. Thereafter, they were removed from the solution and washed with water to eliminate the BSA excess.

2.5. Scanning electron microscopy (SEM) and field emission scanning electron microscopy (FESEM)

A Jeol JSM-6300 scanning electron microscope was used to observe the morphology of the samples using an acceleration voltage of 20 kV. Samples were coated with Au using a Sputter Coater Bal-Tec SCD 005. A Zeiss Ultra 55 FESEM was used to observe the morphology of samples submitted to rubbing fastness tests using an acceleration voltage of 3 kV.

2.6. Atomic force microscopy (AFM)

Atomic force microscopy (AFM) was used to determine surface topography and roughness of the different samples. AFM analyses were performed with a multimode AFM microscope with a Nanoscope® IIIa ADCS controller (Veeco Metrology Group). A monolithic silicon cantilever (FESP, tip radius 8 nm, Bruker AFM probes) with a constant force of 2.8 N/m and a resonance frequency of 75 kHz was used to work on tapping mode. Roughness was evaluated from the analysis of the section.

2.7. Electrochemical impedance spectroscopy measurements

An Autolab PGSTAT302 potentiostat/galvanostat was used to perform EIS analyses. EIS measurements were performed in the 10^{5}-10^{-2} Hz frequency range. The amplitude of the sinusoidal voltage used was ± 10 mV. Measurements were carried out in a two-electrode arrangement, where the sample was located between two round copper electrodes (A = 1.33 cm^{2}).

2.8. Rubbing fastness tests

Rubbing fastness tests were performed to quantify the resistance of the RGO coatings to physical action. Rubbing fastness tests of RGO coated fabrics were performed as explained in the norm ISO 105-X12:2001. Each sample was abraded against cotton abrasive fabric for ten cycles. The change in the resistance of the fabrics after performing the rubbing fastness tests was measured using a Goldstar Digital Multimeter (DM-311). Ten measurements were averaged for each sample analyzed. Field emission scanning electron microscopy (FESEM) was also used to observe the morphology of the conductive fabrics before and after performing the rubbing fastness tests.

2.9. Scanning electrochemical microscopy (SECM)

SECM measurements were carried out with a scanning electrochemical microscope (Sensolytics). A three-electrode configuration cell consisting of a 100-μm-diameter Pt microelectrode, a Pt wire auxiliary electrode, and an Ag/AgCl (3 M KCl) reference electrode. Measurements were performed in $K_3Fe(CN)_6$ 0.01 M and 0.1 M KCl (supporting electrolyte). All the experiments were carried out in an inert nitrogen atmosphere. The substrates were samples (0.5 x 0.5 cm^2) cut from different fabrics (PES, PES-1G, PES-3G, PES-5G, PES-10G, PES-plasma-BSA-1G). These samples were glued to microscope slides with epoxy resin. The microelectrode operated at a potential of 0 V, at which the oxidized form of the redox mediator (Ox) is reduced (Red) at a diffusion controlled rate. Approaching curves were obtained by recording the tip reduction current as the Pt microelectrode tip was moved in direction z. Approaching curves give an indication of the electroactivity of the surface. These curves were

compared to the theoretical curves (positive and negative feedback models). The substrate surfaces for all the measurements were at their open circuit potential (OCP).

3. Results and discussion

3.1.Contact angle measurements and surface energy

Plasma technique was employed to modify the hydrophilicity of the fabric by increasing the plasma dosage applied ($W \cdot min \cdot m^{-2}$). ~~Contact angle measurements were performed with a goniometer.~~ Table 2 shows the static contact angle (º) obtained on the surface of plasma treated polyester fabrics with various liquids (water, glycerol and polyethylene glycol). The surface energy ($mJ \cdot m^{-2}$) was also calculated using the Wu method [36]. Untreated polyester fabric presented a contact angle of 130º when measured with water. With the plasma treatment; there was a decrease of the contact angle due to the increasing hydrophilicity of the plasma treated fabrics. The plasma treatment created polar groups on the surface of the fabric, due to the incorporation of O and N from the air since DBD uses air as gas discharge [30]. Firstly, the plasma treatment creates radicals on the surface of polyester fabrics due to the rupture of ester bonds [31]. These radicals react with the plasma gas generated and produce polar groups such as C-O, C=O, C=N, C≡N and N-C-O [30]. These polar groups allow the formation of dipolar interactions, van der Waals forces, or hydrogen bonds between the fabric and the coating, thereby increasing the adhesion of the coating to the surface of the fabric [30]. The functional groups created are prone to suffer an ageing process due to the reorganization of the surface polar groups that tend to bury themselves below the surface [37, 38]. This is why BSA and RGO coatings were subsequently applied to avoid the loss of efficiency of the plasma treatment.

As can be seen in Table 2, there is a stabilization of the contact angles as well as the surface energy for a plasma dosage of 3000 $W \cdot min \cdot m^{-2}$. Higher plasma dosages produce little variation in these properties but increase energy consumption. There is an equilibrium between the creation of functional groups and removal by the plasma application, it should be taken into account that the plasma application produces the elimination of material from the substrate surface. At a certain plasma dosage (depending on the type of plasma, conditions, and substrate) equilibrium is achieved and higher plasma dosages do not produce an increase in functional groups nor an increase in roughness. This is why the plasma dosage of 3000 $W \cdot min \cdot m^{-2}$ was selected as the optimum plasma dosage to treat the polyester fabrics.

The plasma treatment also produces the removal of grease and contamination from the surface of the fabric. The presence of grease tends to increase the contact angle value and its removal produces a cleaning of the fabric surface, and the subsequent decrease of the contact angle [39]. The measurement of the contact angle in fabrics is somehow limited due to its irregular and porous nature. This is why other measurements such as the dynamic contact angle are usually employed as an indication of wettability [39].

Fig. 1 shows the dynamic contact angle (º) obtained for the untreated PES fabric and the PES fabric treated with 500 $W \cdot min \cdot m^{-2}$ plasma dosage. The other samples are not shown since the absorption process was very rapid and only the static contact angle could be obtained. The dynamic contact angle gives an indication of the wettability of the surface. The initial value of the dynamic contact angle corresponds to the value of the static contact angle – the water drop then begins to be absorbed, the contact angle is progressively reduced, and the drop is finally totally absorbed. As can be seen, there is an improvement in the wettability with the plasma treatment. This improvement has been attributed to the creation of polar groups and microporosity [40-42].

3.2. Atomic force microscopy (AFM) of plasma treated fabrics

Atomic force microscopy (AFM) was used to observe the surface topography of untreated and plasma treated PES samples. SEM has insufficient vertical resolution to observe the change in the roughness caused by the plasma treatment; this is why AFM was employed for this purpose [30]. Another advantage, when compared to the SEM technique, is that the samples are not coated with Au or C and there is no addition of material to the samples. Fig. 2 shows the AFM 3D representations of PES fibers treated with different plasma dosages (0, 500, 3000 and 7500 $W \cdot min \cdot m^{-2}$). Fig. 2-a shows the representation of untreated PES fiber; as can be seen the fiber is quite smooth with no remarkable features. When the PES fibers were treated with a plasma dosage of 500 $W \cdot min \cdot m^{-2}$ (Fig. 2-b) there was an increase in the roughness of the fibers. With an optimum plasma dosage of 3000 $W \cdot min \cdot m^{-2}$ (Fig. 2-c) the roughness of the PES fibers again increased. However, with the highest plasma dosage applied (7500 $W \cdot min \cdot m^{-2}$) there was no substantial increase in the surface roughness (Fig. 2-d) when compared with the 3000 $W \cdot min \cdot m^{-2}$ plasma dosage (Fig. 2-c). These results are in agreement with the surface energy values, which showed stabilization with a dosage of 3000 $W \cdot min \cdot m^{-2}$ as optimal.

Fig. 3 shows the AFM 2D representation of PES fibers treated with different plasma dosages (0, 500, 3000 and 7500 $W \cdot min \cdot m^{-2}$). In the images, roughness has also been obtained in the section represented by the white line in the 2D images. The comparison of the section roughness profiles with the plasma dosages applied are shown in Fig. 3-e. Fig. 3-a shows the 2D representation of the untreated PES fiber. When the PES fabrics were treated with 500 $W \cdot min \cdot m^{-2}$ (Fig. 3-b) there was an increase in roughness, indicated by the presence of white spots in the image. Figures 3-c and 3-d show the

representation of PES fabric treated with 3000 and 7500 $W \cdot min \cdot m^{-2}$, respectively. Both images are similar, which indicates similar levels of roughness. This can also be seen in the section roughness profiles in Fig. 3-e. The values of roughness (Rz) obtained for the samples of PES treated with plasma dosages of 0, 500, 3000 and 7500 $W \cdot min \cdot m^{-2}$ were: 2.747; 8.497; 19.285; and 22.454 nm; respectively. These values again confirm the stabilization of the roughness with a plasma dosage of 3000 $W \cdot min \cdot m^{-2}$.

3.3. Scanning electron microscopy (SEM) and atomic force microscopy (AFM) of PES-RGO conductive fabrics

Scanning electron microscopy (SEM) was employed to observe the morphology of the conductive fabrics. PES fabrics coated with a different number of RGO coatings were obtained to compare the results with the samples treated with plasma and coated with BSA and RGO. Fig. 4-a shows the fabric coated with one RGO coating. Some RGO particles can be observed on the PES fibers. It is difficult to observe the RGO sheets on the surface of the fibers and only the wrinkles of the RGO sheets help to locate them [21,22]. When the number of RGO coatings applied increased (Fig. 4-b shows the fabric coated with three RGO coatings), the presence of more RGO particles was observed. In Fig. 4-c the fabric coated with five RGO coatings is shown, in this image one RGO sheet can be observed in the center of the image connecting two fibers. The RGO sheet is approximately 25 µm x 25 µm. In this case, there was a substantial increase in the level of coating represented by an increase in the number of particles observed. In Fig. 4-d a fabric coated with ten RGO layers is shown and an increase in the RGO coating was observed. In general, there was an increase in the level of coating of the fibers with an increasing number of RGO coatings.

Fig. 5 shows various micrographs of PES treated with plasma (3000 $W \cdot min \cdot m^{-2}$) and coated with BSA and one RGO layer. By observing the figures, it can be seen that the fabrics have been coated with RGO.

Atomic force microscopy was also employed to characterize the sample of PES treated with plasma 3000 $W \cdot min \cdot m^{-2}$ and coated with BSA and one layer of RGO (Fig. 6). If the 3D and 2D AFM images are compared with the AFM images of the PES fabric treated with 3000 $W \cdot min \cdot m^{-2}$ (Fig. 2-c and Fig. 3-c), a substantial change in the roughness of the sample can be seen. The roughness produced by the plasma treatment is no longer observed since BSA and RGO are deposited on the surface of the fiber. The typical morphology of RGO sheets with its wrinkles [21, 22, 43] can be observed in the 3D and 2D AFM representations. The section roughness profile is also shown in Fig. 6-c, and as can be seen, the roughness was substantially reduced when compared with the section profile of plasma treated fabric (Fig. 3-e).

3.4.Electrochemical impedance spectroscopy (EIS)

Electrochemical impedance spectroscopy (EIS) was used to measure the electrical properties of the different conducting fabrics. EIS enables the measurement of electrical resistance and in addition the phase angle; which gives an indication of the conducting/insulating behavior of the fabrics [10, 11, 21, 22]. Table 3 shows the values of impedance modulus |Z| obtained for the different fabrics and treatments applied. Fig. 7 shows the Bode plots for the characterization of conducting fabrics of PES coated with a different number of RGO layers (1, 3, 5, 10). The characterization of PES fabric and PES coated with GO is also shown as a reference. Fig. 7-a shows the plot of the impedance modulus |Z| vs. the frequency (Hz). PES fabric presented values of

impedance modulus |Z| higher than 10^{11} Ω. When PES was coated with GO, there was no substantial variation in the value of |Z|. GO is an electrically insulating material because of the disrupted sp^2 structure due to the presence of oxidized groups [41]. When GO was chemically reduced to RGO, there was a decrease of around five orders of magnitude in the impedance modulus. This decrease of |Z| is related to the reduction of functional groups and the partial restoration of the graphene sp^2 structure [44-46]. There was a gradual decrease of |Z| when more RGO layers were applied to the fabric. The values of impedance modulus obtained were: 21000 kΩ, 145 Ω, 87 Ω and 9 Ω for PES-1G, PES-3G, PES-5G and PES-10G samples, respectively. The variation of |Z| with the numbers of coatings can be correlated with the higher coating level achieved with more RGO coatings – as SEM micrographs have shown (Fig. 4).

Fig. 7-b shows the representation of the -phase angle vs. the frequency. PES and PES-GO present values of -phase angle near to 90º, this value indicates that these fabrics behave like a capacitor and hence are insulating materials. The data for low frequencies is not shown since noise was observed due to the large values of |Z|. When GO was reduced to RGO, the -phase angle changed to 0º in the low frequency region (<10 Hz). However, in the high frequency region (10^5-10^1 Hz) the values of -phase angle varied from 90º to 0º. When more RGO layers were applied, the -phase angle was 0º in the entire frequency range. This value of -phase angle indicates a resistive behavior of the material which is typical of conducting materials.

Fig. 8 shows the electrical characterization of PES fabrics treated with various plasma dosages (500, 3000 and 7500 $W \cdot min \cdot m^{-2}$) and coated with one RGO layer. As can be seen, all the fabrics present similar behavior to untreated PES. The value of impedance modulus |Z| for low frequencies was around 10^{11} Ω (Fig. 8-a). The explanation for this fact is that the plasma treatment creates negative charges due to the functional groups

created on the surface of the polyester fabric [47]. DBD treatment produced an increase in the O and N content due to their incorporation in functional groups such as C-O, C=O, C=N, C≡N and N-C-O [30]. GO also presented negative charges [25, 48] so there is a repulsion between GO and the surface of the plasma treated PES. The assembly of GO sheets on the surface is not possible and the material presents an insulating behavior. The -phase angle also gives an indication of the conducting/insulating nature of the surface (Fig. 8-b). All the fabrics presented 90º of phase, indicating a capacitive behavior which is typical of insulating materials.

In another experiment, the fabrics treated with different plasma dosages were reduced with a 50 mM solution of $Na_2S_2O_4$ to eliminate the oxidized groups from the surface of the polyester fibers. In Fig. 8, the PES fabric treated with a plasma dosage of 3000 $W \cdot min \cdot m^{-2}$, and reduced and coated with one RGO layer is shown as an example. The untreated PES coated with one RGO layer is also shown for comparison. As can be seen, when plasma treated PES (3000 $W \cdot min \cdot m^{-2}$) was chemically reduced, the negative charges of the surface were removed and the assembly of GO layers on the surface of the fabric was again possible. The value of impedance modulus |Z| obtained for the mentioned sample is 46 times lower than that for untreated PES coated with one RGO layer (460 kΩ vs. 21000 kΩ). The explanation for this fact could be the roughness created on the surface of PES fibers due to the plasma treatment (as observed by AFM). The roughness of the fibers increases the fixation points of GO to PES fibers, increasing the coating level of the fibers and hence diminishing the electrical resistance of the fabrics. A similar trend was observed with the -phase angle (Fig. 8-b) The sample treated with plasma, chemically reduced and coated with RGO presented phase angle values lower than the untreated sample of PES coated with RGO in the high frequency

range (10^1-10^5 Hz). For frequencies lower than 10 Hz, the -phase angle was 0º for both samples.

To produce the assembly of GO sheets on the surface of the plasma treated PES, positive charges should be created on the surface of PES. To create the positive charges, an aqueous solution of bovine serum albumin (BSA) was used [25]. BSA is a protein obtained from blood [49]. The fabrics were put in contact with a 0.5 % weight BSA aqueous solution for 15 min to allow the adsorption of BSA. The BSA coating was applied at different pH (4, 7, 10) on PES fabrics to observe the influence of this parameter. The pH of the BSA solution was adjusted with NaOH and HCl solutions. After this process, the fabrics were rinsed with water to remove the BSA excess. The modified BSA-PES textiles were then coated with RGO following the procedure shown in Section 2.4. Fig. 9 shows the electrical characterization by EIS of the PES-BSA-RGO fabrics. The values of impedance modulus obtained were 73 Ω, 356 Ω, 323 Ω, for pH 7, 4 and 10, respectively. This indicates that the optimal pH to coat the fabrics with RGO is neutral pH. With the plasma treatment, a BSA coating and one RGO coating, the value of |Z| achieved was similar to the value obtained for untreated PES coated with five RGO layers (73 Ω vs. 86.8 Ω, respectively). The plasma treatment and BSA coating increases the coating level of RGO on the fabric (as shown by SEM micrographs). A decrease in the electrical resistance of the conducting fabrics was also observed. To compare results, another PES fabric was coated with BSA and one RGO coating without applying the plasma treatment. The value of impedance modulus obtained was 306 Ω (value situated between 2 and 3 RGO coatings directly applied on PES).

3.5.Scanning electrochemical microscopy (SECM)

The electroactivity of the different RGO coated samples was tested by means of the SECM technique using approaching curves. To record these curves, the microelectrode was polarized at a potential (0 V) with which the oxidized form of the redox mediator (Ox) is reduced (Red) on the microelectrode surface at a diffusion controlled rate (Fig. 10). The measured current is defined as $i_\infty = 4 \cdot n \cdot F \cdot D \cdot C \cdot a$, where n is the number of electrons, F is the Faraday constant, D is the diffusion coefficient, C is the bulk concentration of the redox mediator, and a is the radius of the microelectrode tip. In approaching curves, the normalized current registered at the microelectrode (I) is represented vs. the normalized distance (L). The normalized current is defined as follows: $I = i/i_\infty$ where "i" is the current measured at the UME tip and i_∞ is the diffusion current defined above. The normalized current depends on RG (RG=Rg/a, where Rg is the radius of the insulating glass surrounding the Pt tip of radius "a") and the normalized distance L; where L=d/a (d is the microelectrode-substrate separation). The RG of the microelectrode used in this work was $RG \geq 20$.

Various situations can arise depending on the electroactivity of the substrates and the distance between the microelectrode and the substrate:

- When the microelectrode is sufficiently far from the substrate, the measured current corresponds to the diffusion current (i_∞).
- When the substrate is non-conductive, as the microelectrode approaches the substrate there is a hindrance to the diffusion of Ox species. The surface of the fabric is unable to regenerate (oxidize) the reduced form of the redox mediator (Red), hence there is a decrease in the reduction current on the surface of the microelectrode, $i<i_\infty$. This situation is known as negative feedback [50].
- Conversely, if the substrate is conductive, when the microelectrode approaches the surface, there is an increase of the oxidized redox species flux (Ox) since the

surface potential is able to regenerate (oxidize) the redox mediator. This causes an increase in the current measured at the microelectrode, $i>i_{\infty}$. This case is known as positive feedback [50].

Experimental data was compared with theoretical approaching curves for positive and negative feedback models, according to equations 1 and 2. According to Rajendran *et al*. [51], Pade's approximation gives a close and simple equation with less relative error for all distances and valid for RG > 10. The approximate formula of the steady-state normalized current assuming positive feedback for finite conductive substrate together with finite insulating glass thickness is:

$$I_T{}^{C} = \left[\frac{1 + 1.5647/L + 1.316855/L^2 + 0.4919707/L^3}{1 + 1.1234/L + 0.626395/L^2} \right] \quad (1)$$

The expression for the normalized current (assuming negative feedback) was based on the equation obtained by Bard *et al*., for a RG=20 and L range 0.4-20 [52]:

$$I_T{}^{INS} = \left[\frac{1}{0.3554 + 2.0259/L + 0.62832 \times \exp\left(-2.55622/L\right)} \right] \quad (2)$$

Fig. 11 shows the approaching curves obtained by SECM for the different samples analyzed. The sample of PES-1G shows a slight negative feedback (there is a decrease in the normalized current as the microelectrode approaches the surface of the fabrics). The fabric is not completely coated with RGO and there are also zones that are not coated, but the sample behaves mainly as a non-electroactive material. The zones not coated prevailed over coated zones and negative feedback was obtained, although a pure negative feedback model was not achieved for this reason. When the number of RGO layers increased there was a better coverage of the surface of the fabric and positive feedback was obtained on the whole surface of the fabrics. Significant differences were

not observed between 3, 5 and 10 RGO coatings, since similar values of feedback were achieved. In the SECM technique only the superficial coverage of the fabric has an effect on the electrochemical response obtained. In addition, the interconnection between the different RGO sheets or fibers has no effect; in this case the substrate is not polarized and operates at open circuit potential. On the other hand, in the conductivity measurements by EIS, it is this interconnection that provides the conductive pathways that allow the electrical flow.

When the PES fabric was treated with plasma and coated with BSA and one RGO coating, the fabric presented positive feedback across the whole surface. This indicates that the plasma and BSA coating improves the uniformity of the coating; and with only one RGO layer, a complete coverage of the surface of the fabric was achieved. The creation of functional groups by plasma and the posterior conversion of these negative groups to positive groups by BSA helps to improve the uniformity of the coating. The electroactivity obtained in this case was lower than the sample of PES coated with three RGO layers. This could be due to the presence of more RGO aggregates (electroactive) on the surface of the PES-3G sample.

3.6. Rubbing fastness tests

Rubbing fastness tests were performed in order to test the mechanical resistance of the RGO coatings against abrasion and to see whether there was an improvement in the mechanical resistance with the plasma and BSA treatment. The samples in this case were analyzed with FESEM and no extra coating was applied on the samples. The RGO coating served as conductive material. Taking advantage of this situation, the zones where the coating was removed could be easily identified as whiter zones due to the accumulation of electrons in non-conductive zones. Fig. 12-a, b show the FESEM

micrographs for the sample of PES-plasma-BSA-1G prior to performing the rubbing fastness test. All the fibers were coated with RGO and the presence of RGO aggregates could also be observed (Fig. 12-b). When the rubbing test was performed whiter zones could be observed, which indicated the removal of the RGO coating in these zones (Fig. 12-c, d). The RGO aggregates were also removed from the surface of the fibers due to friction (as can be seen in Fig. 12-d). However, the degradation of the coating was not very high when compared to the PES-5G sample after performing the rubbing fastness test (Fig. 12-e, f). In this case, the appearance of whiter zones due to the removal of the RGO coating was evident and extensive (Fig. 12-e). The degradation of the coating could also be observed with higher magnification (Fig. 12-f), the delamination of the RGO coating could be easily observed. The plasma and BSA treatment improves the adhesion of the RGO layers due to an improvement in the interaction forces between the fibers and coating. The influence of the chemical modification was observed with the fabrics obtained after plasma/BSA treatment. The comparison between the resistance values of the PES-plasma-BSA-1G fabric and the PES-1G fabric showed a value of |Z| of 73 Ω and 20967 kΩ, respectively. This represents a 287,000-fold improvement due to the chemical modification produced with plasma and BSA.

However, the physical modification (created mainly by increased roughness) that enabled an increase in the contact area between PES and RGO seemed to have less influence than the chemical modification. The physical modification influence was observed after chemically reducing a plasma treated fabric in order to eliminate the functional groups that did not allow the assembly of GO. The value of resistance obtained for the PES-plasma-reduced-1G fabric was 460 kΩ vs. 21000 kΩ for the untreated plasma PES-1G fabric, which was a 46-fold improvement.

Clearly, the chemical modification prevails over the physical modification in enhancing the adhesion and uniformity of the coating.

Electrical measurements showed in both cases an increase in the resistance of the fabrics of 7.5 % and 11 % for PES-5G and PES-plasma-BSA-1G, respectively. There was little difference between the sample treated with plasma and BSA and the untreated sample. The explanation for this fact is that the degradation is produced on the uppermost part of the fibers. The other parts of the fibers are still coated with RGO and allow electrical conduction [30].

The fabrics obtained could be employed as antistatic materials [21, 22] and also as support materials for depositing other materials such as nanoparticles:

- Pt nanoparticles for electrocatalysis to exploit the high surface area of the RGO and fabric with application for fuel cells [53, 54].
- Ti nanoparticles for photocatalysis. Self-cleaning textiles have been reported in the bibliography [55]. The combination of TiO_2 and graphene derivatives enhances photocatalytical activity due to an increased recombination time between electron and holes [56, 57]. The combination of TiO_2 and graphene derivatives has not been applied on fabrics to the best of our knowledge. In addition it could be a good way to support the photocatalyst.

More work is in progress to combine RGO fabrics with Pt and TiO_2 nanoparticles and study performance for electrochemical and photocatalytic systems.

4. Conclusions

A plasma technique has been used to increase the surface adhesion of reduced graphene oxide (RGO) on polyester (PES) fabrics. Polyester fabrics were treated with an

atmospheric plasma (dielectric barrier discharge) with different plasma dosages. The surface energy (measured by contact angle measurements) and the surface roughness (measured by atomic force microscopy or AFM) increased with the plasma dosage applied until there was a stabilization with a plasma dosage of 3000 $W \cdot min \cdot m^{-2}$. Higher plasma dosages only produced an increase in energy consumption.

The plasma treatment generated negative charges on the surface of PES, hence the self-assembly of GO on plasma treated PES fabrics was impossible under these conditions since GO also presents negative charges. For this reason, an intermediate coating between GO and PES was employed to generate positive charges on the surface of the fabric and allow the assembly of GO. The coating used for this purpose was the protein bovine serum albumin (BSA).

Scanning electron microscopy (SEM) showed the formation of RGO coatings on the surface of PES fibers. The plasma treatment and BSA coating produced an increase in the coating level on the fabrics when compared with untreated fabrics. AFM also showed the deposition of RGO on the surface of plasma treated fabrics.

The electrical resistance of the fabrics was measured using electrochemical impedance spectroscopy (EIS). The treatment of the fabrics with plasma and BSA produced a decrease in the resistance of the fabrics due to an increase in the coating level of the fabrics. With only one RGO coating, values of resistance similar to the untreated sample of PES coated with five RGO coatings were obtained. The plasma treatment decreased the number of coatings needed to achieve similar values of electrical resistance. This enables a reduced processing time and also a saving in chemical products and water. This would justify the application of the plasma/BSA treatment.

The electroactivity of conductive fabrics was measured with scanning electrochemical microscopy (SECM) using approaching curves. The treatment with plasma and BSA

improved the electroactivity of the fabrics with the application of fewer RGO coatings due to an improved surface coverage.

Mechanical resistance of the coatings was tested by means of rubbing fastness tests. The plasma treatment and BSA coating increased the adhesion of RGO to the surface of PES fibers as FESEM micrographs have shown.

Acknowledgements

The authors wish to thank to the Spanish Ministry of Science and Innovation (contract CTM2011-23583) for their financial support. J. Molina is grateful to the Department of Education, Training and Work (Generalitat Valenciana) for the Programa VALi+D Postdoctoral Fellowship. The Electron Microscopy Service of the UPV (Universitat Politècnica de València) is gratefully acknowledged for helping with FESEM and AFM characterization.

References

[1] A.R. Horrocks, B.K. Kandola, P.J. Davies, S. Zhang, S.A. Padbury, Developments in flame retardant textiles – a review, Polym. Degrad. Stabil. 88 (2005) 3–12.

[2] M. Yu, Z. Wang, H. Liu, S. Xie, J. Wu, H. Jiang, J. Zhang, L. Li, J. Li, Laundering durability of photocatalyzed self-cleaning cotton fabric with TiO_2 nanoparticles covalently immobilized, ACS Appl. Mater. Interfaces 5 (2013) 3697–3703.

[3] Y. Shin, D. Yoo, K. Son, Development of thermoregulating textile materials with microencapsulated phase change materials (PCM). II. Preparation and application of PCM microcapsules, J. Appl. Polym. Sci. 96 (2005) 2005–2010.

[4] R.F. Service, Electronic textiles charge ahead, Science 301 (2003) 909–911.

[5] J.W. Lee, T. Mayer-Gall, K. Opwis, C.E. Song, J.S. Gutmann, B. List, Organotextile catalysis, Science 341 (2013) 1225–1229.

[6] S. Coyle, Y. Wu, K.-T. Lau, D. De Rossi, G. Wallace, D. Diamond, Smart nanotextiles: A review of materials and applications, MRS Bulletin 32 (2007) 434–442.

[7] E. Romero, J. Molina, A.I. del Río, J. Bonastre, F. Cases, Synthesis of PPy/$PW_{12}O_{40}^{3-}$ organic-inorganic hybrid material on polyester yarns and subsequent weaving to obtain conductive fabrics, Text. Res. J. 81 (2011) 1427–1437.

[8] A. Bhattacharyya, M. Joshi, Development of polyurethane based conducting nanocomposite fibers via twin screw extrusion, Fiber. Polym. 12 (2011) 734–740.

[9] A. Kaynak, S.S. Najar, R.C. Foitzik, Conducting nylon, cotton and wool yarns by continuous vapor polymerization of pyrrole, Synth. Met. 158 (2008) 1–5.

[10] J. Molina, J. Fernández, A.I. del Río, R. Lapuente, J. Bonastre, F. Cases, Stability of conducting polyester/polypyrrole fabrics in different pH solutions. Chemical and electrochemical characterization, Polym. Degrad. Stabil. 95 (2010) 2574–2583.

[11] J. Molina, J. Fernández, A.I. del Río, J. Bonastre, F. Cases, Chemical, electrical and electrochemical characterization of hybrid organic/inorganic polypyrrole/$PW_{12}O_{40}^{3-}$ coating deposited on polyester fabrics, Appl. Surf. Sci. 257 (2011) 10056–10064.

[12] K.S. Novoselov, A.K. Geim, S.V. Morozov, D. Jiang, Y. Zhang, S.V. Dubonos, I.V. Grigorieva, A.A. Firsov, Electric field effect in atomically thin carbon films, Science 306 (2004) 666−669.

[13] K.S. Novoselov, V.I. Fal'ko, L. Colombo, P.R. Gellert, M.G. Schwab, K. Kim, A roadmap for graphene, Nature 490 (2012) 192−200.

[14] F. Bonaccorso, Z. Sun, T. Hasan, A.C. Ferrari, Graphene photonics and optoelectronics, Nat. Photonics 4 (2010) 611−622.

[15] A.H. Castro Neto, F. Guinea, N.M.R. Peres, K.S. Novoselov, A.K. Geim, The electronic properties of graphene, Rev. Mod. Phys. 81 (2009) 109−162.

[16] H.B. Heersche, P. Jarillo-Herrero, J.B. Oostinga, L.M.K. Vandersypen, A.F. Morpurgo, Bipolar supercurrent in graphene, Nature 446 (2007) 56−59.

[17] A.N. Grigorenko, M. Polini, K.S. Novoselov, Graphene plasmonics, Nat. Photonics 6 (2012) 749−758.

[18] C. Soldano, A. Mahmood, E. Dujardin, Production, properties and potential of graphene, Carbon 48 (2010) 2127−2150.

[19] V. Singh, D. Joung, L. Zhai, S. Das, S.I. Khondaker, S. Seal, Graphene based materials: Past, present and future, Prog. Mater. Sci. 56 (2011) 1178–1271.

[20] S. Park, R.S. Ruoff, Chemical methods for the production of graphenes, Nat. Nanotechnol. 4 (2009) 217−224.

[21] J. Molina, J. Fernández, J.C. Inés, A.I. del Río, J. Bonastre, F. Cases, Electrochemical characterization of reduced graphene oxide-coated polyester fabrics, Electrochim. Acta 93 (2013) 44–52.

[22] J. Molina, J. Fernández, A.I. del Río, J. Bonastre, F. Cases, Chemical and electrochemical study of fabrics coated with reduced graphene oxide, Appl. Surf. Sci. 279 (2013) 46–54.

[23] M. Shateri-Khalilabad, M.E. Yazdanshenas, Fabricating electroconductive cotton textiles using graphene, Carbohyd. Polym. 96 (2013) 190–195.

[24] M. Shateri-Khalilabad, M.E. Yazdanshenas, Preparation of superhydrophobic electroconductive graphene-coated cotton cellulose, Cellulose 20 (2013) 963–972.

[25] Y.J. Yun, W.G. Hong, W.-J. Kim, Y. Jun, B.H. Kim, A novel method for applying reduced graphene oxide directly to electronic textiles from yarns to fabrics, Adv. Mater. 25 (2013) 5701–5705.

[26] B. Fugetsu, E. Sano, H. Yu, K. Mori, T. Tanaka, Graphene oxide as dyestuffs for the creation of electrically conductive fabrics, Carbon 48 (2010) 3340–3345.

[27] W. Gu, Y. Zhao, Graphene modified cotton textiles, Adv. Mat. Res. 331 (2011) 93−96.

[28] Y.-L. Huang, A. Baji, H.-W. Tien, Y.-K. Yang, S.-Y. Yang, C.-C.M. Ma, H.-Y. Liu, Y.-W. Mai, N.-H. Wang, Self-assembly of graphene onto electrospun polyamide 66 nanofibers as transparent conductive thin films, Nanotechnology 22 (2011) 475603.

[29] G. Yu, L. Hu, M. Vosgueritchian, H. Wang, X. Xie, J.R. McDonough, X. Cui, Y. Cui, Z. Bao, Solution-processed graphene/MnO_2 nanostructured textiles for high-performance electrochemical capacitors, Nano Lett. 11 (2011) 2905–2911.

[30] J. Molina, F. R. Oliveira, A. P. Souto, M. F. Esteves, J. Bonastre, F. Cases, Enhanced adhesion of polypyrrole/$PW_{12}O_{40}^{3-}$ hybrid coatings on polyester fabrics, J. Appl. Polym. Sci. 129 (2013) 422–433.

[31] F. Leroux, C. Campagne, A. Perwuelz, L. Gengembre, Atmospheric air plasma treatment of polyester textile materials. Textile structure influence on surface oxidation and silicon resin adhesion, Surf. Coat. Technol. 203 (2009) 3178–3183.

[32] C.W. Kan, K. Chan, C.W.M. Yuen, M.H.J. Miao, The effect of low temperature plasma on chrome dyeing of wool fibres, J. Mater. Process. Technol. 82 (1998) 122–126.

[33] S. Garg, C. Hurren, A. Kaynak, Improvement of adhesion of conductive polypyrrole coating on wool and polyester fabrics using atmospheric plasma treatment, Synth. Met. 157 (2007) 41–47.

[34] Complete textile glossary, available from: http://www.celaneseacetate.com/textile_glossary_filament_acetate.pdf, 2001. Last accessed 15th November 2012.

[35] N. Carneiro, A.P. Souto, F. Forster, E. Prinz, Patent in internationalization phase (2004)/ patent number PCT/PT2004/000008,2004.

[36] F.R. Oliveira, M. Fernandes, N. Carneiro, A.P. Souto, Functionalization of wool fabric with phase-change materials microcapsules after plasma surface modification, J. Appl. Polym. Sci. 128 (2013) 2638–2647.

[37] C. Riccardi, R. Barni, E. Selli, G. Mazzone, M.R. Massafra, B. Marcandallic, G. Poletti, Surface modification of poly(ethylene terephthalate) fibers induced by radio frequency air plasma treatment, Appl. Surf. Sci. 211 (2003) 386–397.

[38] M.R. Sanchis, V. Blanes, M. Blanes, D. Garcia, R. Balart, Surface modification of low density polyethylene (LDPE) film by low pressure O_2 plasma treatment, Eur. Polym. J. 42 (2006) 1558–1568.

[39] A. Zille, F.R. Oliveira, A.P. Souto, Plasma treatment in textile industry, Plasma Process. Polym. 2014, DOI: 10.1002/ppap.201400052.

[40] J. Yip, K. Chan, K.M. Sin, K.S. Lau, Study of physico-chemical surface treatments on dyeing properties of polyamides. Part 1: Effect of tetrafluoromethane low temperature plasma, Color. Technol. 118 (2002) 26–30.

[41] C. Jia, P. Chen, B. Li, Q. Wang, C. Lu, Q. Yu, Effects of twaron fiber surface treatment by air dielectric barrier discharge plasma on the interfacial adhesion in fiber reinforced composites, Surf. Coat. Technol. 204 (2010) 3668–3675.

[42] L.C.V. Wielen, M. Östenson, P. Gatenholm, A.J. Ragauskas, Surface modification of cellulosic fibers using dielectric-barrier discharge, Carbohyd. Polym. 65 (2006) 179–184.

[43] S. Stankovich, D.A. Dikin, G.H.B. Dommett, K.M. Kohlhaas, E.J. Zimney, E.A. Stach, R.D. Piner, S.T. Nguyen, R.S. Ruoff, Graphene-based composite materials, Nature 440 (2006) 282–286.

[44] D.R. Dreyer, S. Park, C.W. Bielawski, R.S. Ruoff, The chemistry of graphene oxide, Chem. Soc. Rev. 39 (2010) 228–240.

[45] D. Chen, H. Feng, J. Li, Graphene oxide: preparation, functionalization, and electrochemical applications, Chem. Rev. 112 (2012) 6027−6053.

[46] C. Vallés, J.D. Núñez, A.M. Benito, W.K. Maser, Flexible conductive graphene paper obtained by direct and gentle annealing of graphene oxide paper, Carbon 50 (2012) 835−844.

[47] L. Guo, C. Campagne, A. Perwuelz, F. Leroux, Zeta potential and surface physico-chemical properties of atmospheric air-plasma-treated polyester fabrics, Text. Res. J. 79 (2009) 1371–1377.

[48] D. Li, M.B. Müller, S. Gilje, R.B. Kaner, G.G. Wallace, Processable aqueous dispersions of graphene nanosheets, Nat. Nanotechnol. 3 (2008) 101–105.

[49] A. Michnik, K. Michalik, Z. Drzazga, Stability of bovine serum albumin at different pH, J. Therm. Anal. Calorim. 80 (2005) 399–406.

[50] P. Sun, F.O. Laforge, M.V. Mirkin, Scanning electrochemical microscopy in the 21st century, Phys. Chem. Chem. Phys. 9 (2007) 802–823.

[51] L. Rajendran, S.P. Ananthi, Analysis of positive feedback currents at the scanning electrochemical microscope, J. Electroanal. Chem. 561 (2004) 113–118.

[52] A.J. Bard, M.V. Mirkin, Scanning Electrochemical Microscopy, Marcel Dekker Inc., New York, 2001.

[53] J. Molina, J. Fernández, A.I. del Río, J. Bonastre, F. Cases, Synthesis of Pt nanoparticles on electrochemically reduced graphene oxide by potentiostatic and alternate current methods, Mater. Charact. 89 (2014) 56–68.

[54] H. Huang, H. Chen, D. Sun, X. Wang, Graphene nanoplate-Pt composite as a high performance electrocatalyst for direct methanol fuel cells, J Power Sources 204 (2012) 46–52.

[55] N.M. Bedford, A.J. Steckl, Photocatalytic self-cleaning textile fibers by coaxial electrospinning, ACS Appl. Mater. Interfaces 2 (2010) 2448–2455.

[56] X. Cao, G. Tian, Y. Chen, J. Zhou, W. Zhou, C. Tiana, H. Fu, Hierarchical composites of TiO2 nanowire arrays on reduced graphene oxide nanosheets with enhanced photocatalytic hydrogen evolution performance, J. Mater. Chem. A 2 (2014) 4366–4374.

[57] Y. Zhao, D. Zhao, C. Chen, X. Wang, Enhanced photo-reduction and removal of Cr(VI) on reduced grapheme oxide decorated with TiO_2 nanoparticles, J. Colloid Interf. Sci. 405 (2013) 211–217.

Figure captions

Fig. 1. Dynamic contact angle measurements for untreated polyester fabrics and plasma treated polyester fabric with a dosage of 500 $W \cdot min \cdot m^{-2}$.

Fig. 2. AFM 3D representations of polyester treated with different plasma dosages: (a) 0 $W \cdot min \cdot m^{-2}$ (b) 500 $W \cdot min \cdot m^{-2}$, (c) 3000 $W \cdot min \cdot m^{-2}$, (d) 7500 $W \cdot min \cdot m^{-2}$.

Fig. 3. AFM 2D representation of polyester treated with different plasma dosages: (a) 0 $W \cdot min \cdot m^{-2}$ (b) 500 $W \cdot min \cdot m^{-2}$, (c) 3000 $W \cdot min \cdot m^{-2}$, (d) 7500 $W \cdot min \cdot m^{-2}$. (e) Section roughness profiles of the 2D representations shown.

Fig. 4. SEM micrographs of (a) PES-1G (×1000), (b) PES-3G (×1000), (c) PES-5G (×1000) and (d) PES-10G (×1000).

Fig. 5. SEM micrographs of PES treated with plasma 3000 $W \cdot min \cdot m^{-2}$ and coated with BSA and RGO (a) (×2000), (b) (×3500).

Fig. 6. AFM analysis of polyester treated with plasma (3000 $W \cdot min \cdot m^{-2}$) and coated with BSA and one layer of RGO. (a) 3D representation, (b) 2D representation, (c) section roughness profile shown in (b).

Fig. 7. Bode plots for PES coated with a different number of RGO coatings (1, 3, 5 and 10). Samples of PES and PES-GO are also shown as reference. Samples located between two metallic conductors. Frequency range from 10^{5} Hz to 10^{-2} Hz.

Fig. 8. Bode plots for PES treated with different plasma dosages (500, 3000, and 7500 $W \cdot min \cdot m^{-2}$) and coated with one layer of RGO. PES treated with plasma (3000 $W \cdot min \cdot m^{-2}$) and reduced chemically and coated with one layer of RGO, and an untreated PES coated with one layer RGO are also shown for comparison. Samples located between two metallic conductors. Frequency range from 10^{5} Hz to 10^{-2} Hz.

Fig. 9. Bode plots for PES treated with plasma (3000 $W \cdot min \cdot m^{-2}$) without RGO coating and PES treated with the plasma (3000 $W \cdot min \cdot m^{-2}$) and coated with BSA at different pH (4, 7, 10) and coated with one layer of RGO. Samples located between two metallic conductors. Frequency range from 10^{5} Hz to 10^{-2} Hz.

Fig. 10. Cyclic voltammogram obtained with a 100 µm diameter Pt SECM-tip in $K_3Fe(CN)_6$ 0.01 M and 0.1 M KCl solution; scan rate 50 $mV \cdot s^{-1}$.

Fig. 11. Approaching curves for PES-1G, PES-3G, PES-5G, PES-10G, PES-plasma-BSA-1G (continuous lines), theoretical negative feedback model () and theoretical positive feedback model (Δ). Obtained with a 100 µm diameter Pt SECM-tip in $K_3Fe(CN)_6$ 0.01 M and 0.1 M KCl. The tip potential was 0 mV (vs. Ag/AgCl) and the approaching rate was 10 $\mu m \cdot s^{-1}$.

Fig. 12. FESEM micrographs of: a), b) PES-plasma-BSA-1G; c), d) PES-plasma-BSA-1G after rubbing fastness test; e), f) PES-5G after rubbing fastness test.

Table captions

Table 1. Conditions and plasma dosages applied to polyester fabrics.

Table 2. Values of contact angles (º) (water, glycerol and polyethylene glycol) and surface energy values ($mJ \cdot m^{-2}$) for PES treated with different plasma dosages.

Table 3. Values of impedance modulus |Z| obtained for the different fabrics.

Plasma treatment of polyester fabrics to increase the adhesion of reduced graphene oxide

J. Molina,[1,2] J. Fernández,[1] M. Fernandes,[2] A.P. Souto,[2] M.F. Esteves,[2] J. Bonastre,[1] F. Cases[1]*

[1]*Departamento de Ingeniería Textil y Papelera, EPS de Alcoy, Universitat Politècnica de València, Plaza Ferrándiz y Carbonell s/n, 03801 Alcoy, Spain*

[2]*Department of Textile Engineering, University of Minho, Campus de Azurém, 4800-058 Guimarães, Portugal*

Abstract

Polyester (PES) fabrics were treated with plasma to enhance the adhesion of reduced graphene oxide (RGO) and produce conductive fabrics. The surface energy of the plasma treated fabrics was measured using contact angle measurements and showed a stabilization of this parameter with plasma dosages of 3000 $W \cdot min \cdot m^{-2}$. The surface roughness measured by atomic force microscopy (AFM) also showed a stabilization with the same plasma dosage value. The plasma treatment induced negative charges on the surface of the fibers and graphene oxide (GO) also presented negative charges – and so deposition of GO on the surface of the PES fibers was not possible. For this reason, bovine serum albumin (BSA) was employed as an intermediate coating that acquired a positive charge and enabled the self-assembly of GO on plasma treated PES fibers. Electrochemical impedance spectroscopy (EIS) was employed to measure the resistance of the conductive fabrics. The plasma treatment and BSA coating improved the coating level of the samples and hence the conductivity of the fabrics was improved with the

application of fewer RGO layers. RGO adhesion on fabrics was also improved as shown in rubbing fastness tests.

Keywords: dielectric barrier discharge (DBD), adhesion, polyester, reduced graphene oxide, conductive fabrics.

---

* Corresponding author. Fax.: +34 966528438; telephone: +34 966528412.

E-mail addresses: jamopue@doctor.upv.es (J. Molina), jaferse1@posgrado.upv.es (J. Fernández), marta.fernandes@det.uminho.pt (M. Fernandes), souto@det.uminho.pt (A.P. Souto), festeves@det.uminho.pt (M.F. Esteves), joboca@txp.upv.es (J. Bonastre), fjcases@txp.upv.es (F. Cases).

1. Introduction

In the field of textiles there is increasing interest in the development of fabrics with new properties such as: flame resistance [1]; self-cleaning [2]; thermal regulation [3]; electrical conduction [4]; or even catalysis [5]. Among these properties, electrical conductivity has attracted particular attention. Conductive fabrics can be employed for the production of smart textiles with the integration of sensors or various electronic devices [6, 7]. Various approaches can be used to produce conductive fabrics. For instance, the use of metallic fibers inserted in the fabric has been reported; however, the continuous bending and stretching that take place in fabrics produce breakages in the fibers [4]. This is why other approaches have been investigated: the extrusion of fibers with conductive particles such as carbon derivatives [8], or the synthesis of conducting polymer films on the fabrics [9-11].

The discovery of graphene and its derivatives has opened a new era in the field of physics and materials science [12]. The outstanding optical, electronic, thermal and mechanical properties shown by this material have created expectations regarding various possible applications [12-19]. Different methods have been employed for the production of graphene and its derivatives [18-20]. Mechanical exfoliation of graphite crystals was the first method reported by Novoselov *et al. [*12]. Although the quality of graphene produced in this way is excellent; the quantity of graphene that can be obtained is minimal and can only be used for fundamental studies. This is why other methods such as chemical vapor deposition or chemical methods have been continuously developed in response to the increasing demand for graphene materials. Chemical methods have been proposed as a cheaper alternative and with higher production capacity than chemical vapor deposition. One of these methods is the production of graphene oxide (GO) by the oxidation of graphite. The oxidation of graphite allows the exfoliation of graphene oxide layers. However, a reduction step is necessary to convert the insulating GO into conducting reduced graphene oxide (RGO) [20].

Regarding the application of graphene and derivatives to produce conductive fabrics, the most widely employed method has been the adsorption of GO on the fabric or fibers and its posterior reduction to produce RGO [21-28]. Graphene oxide sheets are adsorbed on the surface of the fabrics due to the attraction forces between the oxidized groups of GO and the functional groups of the fabrics. The direct deposition of graphene on fabrics has also been reported by Yu *et al*. [29]. In the present paper the adsorption/reduction strategy has been employed to produce RGO coated polyester fabrics. Plasma techniques have been widely used to increase the adhesion between different materials, including polymers [30]. Plasma treatment produces reactive groups

and radicals on the surface of treated fabrics. In the case of polyester, plasma treatment can oxidize the polyester surface by breaking the ester bonds and creating radicals [31]. These radicals are able to react with the plasma gas generated and create hydroxyl, carbonyl, and carboxyl groups. These polar groups form dipolar interactions, van der Waals forces or hydrogen bonds between the fabric and the coating, thereby increasing the adhesion of the coating to the surface of the fabric [30, 32]. In addition to the creation of functional groups, an increase in roughness on the surface of the fabrics takes place due to the removal of material. The rougher surface allows a better contact between the fibers and the coating and enhances its adhesion [30, 31]. The novelty of the paper is the increase in the adhesion of RGO sheets to the surface of the fabrics after applying a plasma technique. The plasma treatment was combined with a bovine serum albumin (BSA) intermediate layer that converted the negative charges generated by plasma treatment on the fabric surface into positive charges, this allowed self-assembly with GO sheets that possess a negative charge before the reduction to RGO. The effect of this treatment on the electrical resistance of the modified fabrics will also be explored.

There are various plasma methods available. In the present work we have used dielectric barrier discharge (DBD). This technique is a type of cold plasma generated by an electric discharge in atmospheric conditions. Electrical discharge takes place between two electrodes separated by a small gap where the fabric is continuously treated at a controlled speed. Fabric modification by plasma methods has the advantage that no water or other chemical products are needed. The low temperature produced by DBD also allows little deterioration of organic samples [33].

2. Experimental

2.1. Reagents and materials

All the reagents used were of analytical grade.

For the synthesis: monolayer graphene oxide (GO) powders were acquired from Nanoinnova Technologies SL (Spain); sodium dithionite ($Na_2S_2O_4$) was acquired from Merck; and bovine serum albumin (BSA) was acquired from Sigma Aldrich. The polyester fabric characteristics were: fabric surface density, 100 $g \cdot m^{-2}$; warp threads per cm, 55; weft threads per cm, 29. These are specific terms used in the textile industry and their meaning can be consulted in a textile glossary [34].

For the characterization: sulphuric acid (H_2SO_4) and potassium chloride (KCl) were purchased from Merck. $K_3Fe(CN)_6$ 99% was used as received from Acrōs Organics.

When needed, solutions were deoxygenated by bubbling nitrogen (N_2 premier X50S). Ultrapure water was obtained from an Elix 3 Millipore-Milli-Q Advantage A10 system with a resistivity of nearly 18.2 MΩ·cm.

2.2. Dielectric barrier discharge (DBD) treatment

Plasma treatment of polyester was carried out at atmospheric pressure with the dielectric barrier discharge modality (DBD) (Softal/University of Minho patented prototype) [35]. The laboratorial prototype machine used in this work has a width of 50 cm and consisted of the following components: a metallic electrode coated with ceramic; a metallic counter electrode coated with silicone; an electric generator and a high tension transformer. The velocity (v) and power (P) are variable and the fabric passed through the electrodes continuously. The plasma dosage was defined by the equation (1) [35]:

$$dosage = \frac{N \cdot P}{v \cdot w} \qquad (1)$$

Where: N (number of passages); P (power, W); v (velocity, $m \cdot min^{-1}$); and w (width, 0.5 m). For the treatment of polyester fabrics, velocity and power were maintained constant and the number of passages was varied. Table 1 shows the conditions created for the treatments.

2.3. Contact angle measurements

For measuring the contact angles of the water drops in untreated and plasma treated polyester fabrics we used Goniometer Dataphysics equipment and OCA software with a video system for the caption of images in static and dynamic modes. A drop of 5 µl of distilled water was placed on the fabric surface with a microliter syringe and observed with a special CCD camera. At least ten measurements at different places were taken for each fabric. The camera takes an image every 0.04 sec.

To calculate the surface energy (γ) and its polar (γ^P) and dispersive components (γ^D) the Wu method (harmonic-mean) was used [36]. The surface energy (γ) is considered to be composed of polar and dispersive components. In particular, the polar component results from three different intermolecular forces due to permanent and induced dipoles and hydrogen bonding, whereas the dispersion (non-polar) component is due to instantaneous dipole moments. For polar solids or liquids, the total γ is a sum of the always-existing London dispersion forces (γ^D) with intermolecular interactions that depend on the chemical nature of the material, compiled as polar forces (γ^P):

$$\gamma = \gamma^D + \gamma^P \quad (2)$$

The polar and dispersive components of the surface energy (γ^D and γ^P, respectively) were calculated using the Wu method (harmonic mean) in equation 3:

$$\gamma_{sl} = \gamma_s + \gamma_l - 4\left[\frac{\gamma_s^D \gamma_l^D}{\gamma_s^D + \gamma_l^D} + \frac{\gamma_s^P \gamma_l^P}{\gamma_s^P + \gamma_l^P}\right] \quad (3)$$

Three liquids with known surface energy and surface energy components were used in this study to calculate the surface energy components of the fabrics: distilled water (γ: 72.8; γ^D: 29.1; γ^P: 43.7); polyethylene glycol 200 (PEG) (γ: 43.5; γ^D: 29.9; γ^P: 13.6); and glycerol (γ: 63.4; γ^D: 37.4; γ^P: 26.0). The units used are $mJ \cdot m^{-2}$.

2.4. Synthesis of reduced graphene oxide on polyester fabrics

Polyester fabrics were coated with reduced graphene oxide (RGO) similar to Fugetsu *et al.* [26]. A 3 g L^{-1} GO solution was obtained sonicating GO monolayer powders in an ultrasound bath for 60 min. The first stage of the synthesis was carried out by putting the GO solution in contact with the fabric to allow the adsorption of GO sheets on the surface of the fabrics. This stage lasted 60 minutes. The fabrics with GO were then dried for 24 h under ambient conditions. The second stage of the synthesis was the reduction of GO to RGO. Fabrics coated with GO were placed for 30 min in a solution containing the reducer (50 mM $Na_2S_2O_4$) at approximately 90º C. Samples with a different number of RGO coatings (1 to 10) were obtained (PES-1G to PES-10G) repeating the procedure mentioned above. The samples treated with plasma were also coated with RGO following the same procedure. The plasma treatment generates negative charges on the surface of the fabrics, GO also presents negative charges so the deposition of GO on the fabrics is not possible under these conditions. For this reason, bovine serum albumin (BSA) was employed as an intermediate coating as it acquires a positive charge and allows the deposition of GO on the surface of the fabrics. A 0.5 % weight aqueous BSA solution [25] prepared at room temperature was employed to coat the plasma treated PES samples. Fabrics were placed in contact with the solution at room temperature for 15 minutes with magnetic stirring. Thereafter, they were removed from the solution and washed with water to eliminate the BSA excess.

2.5. Scanning electron microscopy (SEM) and field emission scanning electron microscopy (FESEM)

A Jeol JSM-6300 scanning electron microscope was used to observe the morphology of the samples using an acceleration voltage of 20 kV. Samples were coated with Au using a Sputter Coater Bal-Tec SCD 005. A Zeiss Ultra 55 FESEM was used to observe the morphology of samples submitted to rubbing fastness tests using an acceleration voltage of 3 kV.

2.6. Atomic force microscopy (AFM)

Atomic force microscopy (AFM) was used to determine surface topography and roughness of the different samples. AFM analyses were performed with a multimode AFM microscope with a Nanoscope® IIIa ADCS controller (Veeco Metrology Group). A monolithic silicon cantilever (FESP, tip radius 8 nm, Bruker AFM probes) with a constant force of 2.8 N/m and a resonance frequency of 75 kHz was used to work on tapping mode. Roughness was evaluated from the analysis of the section.

2.7. Electrochemical impedance spectroscopy measurements

An Autolab PGSTAT302 potentiostat/galvanostat was used to perform EIS analyses. EIS measurements were performed in the 10^{5}-10^{-2} Hz frequency range. The amplitude of the sinusoidal voltage used was ± 10 mV. Measurements were carried out in a two-electrode arrangement, where the sample was located between two round copper electrodes (A = 1.33 cm^{2}).

2.8. Rubbing fastness tests

Rubbing fastness tests were performed to quantify the resistance of the RGO coatings to physical action. Rubbing fastness tests of RGO coated fabrics were performed as explained in the norm ISO 105-X12:2001. Each sample was abraded against cotton abrasive fabric for ten cycles. The change in the resistance of the fabrics after performing the rubbing fastness tests was measured using a Goldstar Digital Multimeter (DM-311). Ten measurements were averaged for each sample analyzed. Field emission scanning electron microscopy (FESEM) was also used to observe the morphology of the conductive fabrics before and after performing the rubbing fastness tests.

2.9. Scanning electrochemical microscopy (SECM)

SECM measurements were carried out with a scanning electrochemical microscope (Sensolytics). A three-electrode configuration cell consisting of a 100-μm-diameter Pt microelectrode, a Pt wire auxiliary electrode, and an Ag/AgCl (3 M KCl) reference electrode. Measurements were performed in $K_3Fe(CN)_6$ 0.01 M and 0.1 M KCl (supporting electrolyte). All the experiments were carried out in an inert nitrogen atmosphere. The substrates were samples (0.5 x 0.5 cm^2) cut from different fabrics (PES, PES-1G, PES-3G, PES-5G, PES-10G, PES-plasma-BSA-1G). These samples were glued to microscope slides with epoxy resin. The microelectrode operated at a potential of 0 V, at which the oxidized form of the redox mediator (Ox) is reduced (Red) at a diffusion controlled rate. Approaching curves were obtained by recording the tip reduction current as the Pt microelectrode tip was moved in direction z. Approaching curves give an indication of the electroactivity of the surface. These curves were compared to the theoretical curves (positive and negative feedback models). The substrate surfaces for all the measurements were at their open circuit potential (OCP).

3. Results and discussion

3.1.Contact angle measurements and surface energy

Plasma technique was employed to modify the hydrophilicity of the fabric by increasing the plasma dosage applied ($W \cdot min \cdot m^{-2}$). Table 2 shows the static contact angle (º) obtained on the surface of plasma treated polyester fabrics with various liquids (water, glycerol and polyethylene glycol). The surface energy ($mJ \cdot m^{-2}$) was also calculated using the Wu method [36]. Untreated polyester fabric presented a contact angle of 130º when measured with water. With the plasma treatment; there was a decrease of the contact angle due to the increasing hydrophilicity of the plasma treated fabrics. The plasma treatment created polar groups on the surface of the fabric, due to the incorporation of O and N from the air since DBD uses air as gas discharge [30]. Firstly, the plasma treatment creates radicals on the surface of polyester fabrics due to the rupture of ester bonds [31]. These radicals react with the plasma gas generated and produce polar groups such as C-O, C=O, C=N, C≡N and N-C-O [30]. These polar groups allow the formation of dipolar interactions, van der Waals forces, or hydrogen bonds between the fabric and the coating, thereby increasing the adhesion of the coating to the surface of the fabric [30]. The functional groups created are prone to suffer an ageing process due to the reorganization of the surface polar groups that tend to bury themselves below the surface [37, 38]. This is why BSA and RGO coatings were subsequently applied to avoid the loss of efficiency of the plasma treatment.

As can be seen in Table 2, there is a stabilization of the contact angles as well as the surface energy for a plasma dosage of 3000 $W \cdot min \cdot m^{-2}$. Higher plasma dosages produce little variation in these properties but increase energy consumption. There is an equilibrium between the creation of functional groups and removal by the plasma

application, it should be taken into account that the plasma application produces the elimination of material from the substrate surface. At a certain plasma dosage (depending on the type of plasma, conditions, and substrate) equilibrium is achieved and higher plasma dosages do not produce an increase in functional groups nor an increase in roughness. This is why the plasma dosage of 3000 $W \cdot min \cdot m^{-2}$ was selected as the optimum plasma dosage to treat the polyester fabrics.

The plasma treatment also produces the removal of grease and contamination from the surface of the fabric. The presence of grease tends to increase the contact angle value and its removal produces a cleaning of the fabric surface, and the subsequent decrease of the contact angle [39]. The measurement of the contact angle in fabrics is somehow limited due to its irregular and porous nature. This is why other measurements such as the dynamic contact angle are usually employed as an indication of wettability [39].

Fig. 1 shows the dynamic contact angle (º) obtained for the untreated PES fabric and the PES fabric treated with 500 $W \cdot min \cdot m^{-2}$ plasma dosage. The other samples are not shown since the absorption process was very rapid and only the static contact angle could be obtained. The dynamic contact angle gives an indication of the wettability of the surface. The initial value of the dynamic contact angle corresponds to the value of the static contact angle – the water drop then begins to be absorbed, the contact angle is progressively reduced, and the drop is finally totally absorbed. As can be seen, there is an improvement in the wettability with the plasma treatment. This improvement has been attributed to the creation of polar groups and microporosity [40-42].

3.2. Atomic force microscopy (AFM) of plasma treated fabrics

Atomic force microscopy (AFM) was used to observe the surface topography of untreated and plasma treated PES samples. SEM has insufficient vertical resolution to

observe the change in the roughness caused by the plasma treatment; this is why AFM was employed for this purpose [30]. Another advantage, when compared to the SEM technique, is that the samples are not coated with Au or C and there is no addition of material to the samples. Fig. 2 shows the AFM 3D representations of PES fibers treated with different plasma dosages (0, 500, 3000 and 7500 $W \cdot min \cdot m^{-2}$). Fig. 2-a shows the representation of untreated PES fiber; as can be seen the fiber is quite smooth with no remarkable features. When the PES fibers were treated with a plasma dosage of 500 $W \cdot min \cdot m^{-2}$ (Fig. 2-b) there was an increase in the roughness of the fibers. With an optimum plasma dosage of 3000 $W \cdot min \cdot m^{-2}$ (Fig. 2-c) the roughness of the PES fibers again increased. However, with the highest plasma dosage applied (7500 $W \cdot min \cdot m^{-2}$) there was no substantial increase in the surface roughness (Fig. 2-d) when compared with the 3000 $W \cdot min \cdot m^{-2}$ plasma dosage (Fig. 2-c). These results are in agreement with the surface energy values, which showed stabilization with a dosage of 3000 $W \cdot min \cdot m^{-2}$ as optimal.

Fig. 3 shows the AFM 2D representation of PES fibers treated with different plasma dosages (0, 500, 3000 and 7500 $W \cdot min \cdot m^{-2}$). In the images, roughness has also been obtained in the section represented by the white line in the 2D images. The comparison of the section roughness profiles with the plasma dosages applied are shown in Fig. 3-e. Fig. 3-a shows the 2D representation of the untreated PES fiber. When the PES fabrics were treated with 500 $W \cdot min \cdot m^{-2}$ (Fig. 3-b) there was an increase in roughness, indicated by the presence of white spots in the image. Figures 3-c and 3-d show the representation of PES fabric treated with 3000 and 7500 $W \cdot min \cdot m^{-2}$, respectively. Both images are similar, which indicates similar levels of roughness. This can also be seen in the section roughness profiles in Fig. 3-e. The values of roughness (Rz) obtained for the samples of PES treated with plasma dosages of 0, 500, 3000 and 7500 $W \cdot min \cdot m^{-2}$ were:

2.747; 8.497; 19.285; and 22.454 nm; respectively. These values again confirm the stabilization of the roughness with a plasma dosage of 3000 $W \cdot min \cdot m^{-2}$.

3.3. Scanning electron microscopy (SEM) and atomic force microscopy (AFM) of PES-RGO conductive fabrics

Scanning electron microscopy (SEM) was employed to observe the morphology of the conductive fabrics. PES fabrics coated with a different number of RGO coatings were obtained to compare the results with the samples treated with plasma and coated with BSA and RGO. Fig. 4-a shows the fabric coated with one RGO coating. Some RGO particles can be observed on the PES fibers. It is difficult to observe the RGO sheets on the surface of the fibers and only the wrinkles of the RGO sheets help to locate them [21,22]. When the number of RGO coatings applied increased (Fig. 4-b shows the fabric coated with three RGO coatings), the presence of more RGO particles was observed. In Fig. 4-c the fabric coated with five RGO coatings is shown, in this image one RGO sheet can be observed in the center of the image connecting two fibers. The RGO sheet is approximately 25 µm x 25 µm. In this case, there was a substantial increase in the level of coating represented by an increase in the number of particles observed. In Fig. 4-d a fabric coated with ten RGO layers is shown and an increase in the RGO coating was observed. In general, there was an increase in the level of coating of the fibers with an increasing number of RGO coatings.

Fig. 5 shows various micrographs of PES treated with plasma (3000 $W \cdot min \cdot m^{-2}$) and coated with BSA and one RGO layer. By observing the figures, it can be seen that the fabrics have been coated with RGO.

Atomic force microscopy was also employed to characterize the sample of PES treated with plasma 3000 $W \cdot min \cdot m^{-2}$ and coated with BSA and one layer of RGO (Fig. 6). If

the 3D and 2D AFM images are compared with the AFM images of the PES fabric treated with 3000 $W \cdot min \cdot m^{-2}$ (Fig. 2-c and Fig. 3-c), a substantial change in the roughness of the sample can be seen. The roughness produced by the plasma treatment is no longer observed since BSA and RGO are deposited on the surface of the fiber. The typical morphology of RGO sheets with its wrinkles [21, 22, 43] can be observed in the 3D and 2D AFM representations. The section roughness profile is also shown in Fig. 6-c, and as can be seen, the roughness was substantially reduced when compared with the section profile of plasma treated fabric (Fig. 3-e).

3.4.Electrochemical impedance spectroscopy (EIS)

Electrochemical impedance spectroscopy (EIS) was used to measure the electrical properties of the different conducting fabrics. EIS enables the measurement of electrical resistance and in addition the phase angle; which gives an indication of the conducting/insulating behavior of the fabrics [10, 11, 21, 22]. Table 3 shows the values of impedance modulus |Z| obtained for the different fabrics and treatments applied. Fig. 7 shows the Bode plots for the characterization of conducting fabrics of PES coated with a different number of RGO layers (1, 3, 5, 10). The characterization of PES fabric and PES coated with GO is also shown as a reference. Fig. 7-a shows the plot of the impedance modulus |Z| vs. the frequency (Hz). PES fabric presented values of impedance modulus |Z| higher than 10^{11} Ω. When PES was coated with GO, there was no substantial variation in the value of |Z|. GO is an electrically insulating material because of the disrupted sp^2 structure due to the presence of oxidized groups [41]. When GO was chemically reduced to RGO, there was a decrease of around five orders of magnitude in the impedance modulus. This decrease of |Z| is related to the reduction of functional groups and the partial restoration of the graphene sp^2 structure [44-46]. There

was a gradual decrease of |Z| when more RGO layers were applied to the fabric. The values of impedance modulus obtained were: 21000 kΩ, 145 Ω, 87 Ω and 9 Ω for PES-1G, PES-3G, PES-5G and PES-10G samples, respectively. The variation of |Z| with the numbers of coatings can be correlated with the higher coating level achieved with more RGO coatings – as SEM micrographs have shown (Fig. 4).

Fig. 7-b shows the representation of the -phase angle vs. the frequency. PES and PES-GO present values of -phase angle near to 90º, this value indicates that these fabrics behave like a capacitor and hence are insulating materials. The data for low frequencies is not shown since noise was observed due to the large values of |Z|. When GO was reduced to RGO, the -phase angle changed to 0º in the low frequency region (<10 Hz). However, in the high frequency region (10^5-10^1 Hz) the values of -phase angle varied from 90º to 0º. When more RGO layers were applied, the -phase angle was 0º in the entire frequency range. This value of -phase angle indicates a resistive behavior of the material which is typical of conducting materials.

Fig. 8 shows the electrical characterization of PES fabrics treated with various plasma dosages (500, 3000 and 7500 $W \cdot min \cdot m^{-2}$) and coated with one RGO layer. As can be seen, all the fabrics present similar behavior to untreated PES. The value of impedance modulus |Z| for low frequencies was around 10^{11} Ω (Fig. 8-a). The explanation for this fact is that the plasma treatment creates negative charges due to the functional groups created on the surface of the polyester fabric [47]. DBD treatment produced an increase in the O and N content due to their incorporation in functional groups such as C-O, C=O, C=N, C≡N and N-C-O [30]. GO also presented negative charges [25, 48] so there is a repulsion between GO and the surface of the plasma treated PES. The assembly of GO sheets on the surface is not possible and the material presents an insulating behavior. The -phase angle also gives an indication of the conducting/insulating nature

of the surface (Fig. 8-b). All the fabrics presented 90º of phase, indicating a capacitive behavior which is typical of insulating materials.

In another experiment, the fabrics treated with different plasma dosages were reduced with a 50 mM solution of $Na_2S_2O_4$ to eliminate the oxidized groups from the surface of the polyester fibers. In Fig. 8, the PES fabric treated with a plasma dosage of 3000 $W \cdot min \cdot m^{-2}$, and reduced and coated with one RGO layer is shown as an example. The untreated PES coated with one RGO layer is also shown for comparison. As can be seen, when plasma treated PES (3000 $W \cdot min \cdot m^{-2}$) was chemically reduced, the negative charges of the surface were removed and the assembly of GO layers on the surface of the fabric was again possible. The value of impedance modulus |Z| obtained for the mentioned sample is 46 times lower than that for untreated PES coated with one RGO layer (460 kΩ vs. 21000 kΩ). The explanation for this fact could be the roughness created on the surface of PES fibers due to the plasma treatment (as observed by AFM). The roughness of the fibers increases the fixation points of GO to PES fibers, increasing the coating level of the fibers and hence diminishing the electrical resistance of the fabrics. A similar trend was observed with the -phase angle (Fig. 8-b) The sample treated with plasma, chemically reduced and coated with RGO presented phase angle values lower than the untreated sample of PES coated with RGO in the high frequency range (10^1-10^5 Hz). For frequencies lower than 10 Hz, the -phase angle was 0º for both samples.

To produce the assembly of GO sheets on the surface of the plasma treated PES, positive charges should be created on the surface of PES. To create the positive charges, an aqueous solution of bovine serum albumin (BSA) was used [25]. BSA is a protein obtained from blood [49]. The fabrics were put in contact with a 0.5 % weight BSA aqueous solution for 15 min to allow the adsorption of BSA. The BSA coating was

applied at different pH (4, 7, 10) on PES fabrics to observe the influence of this parameter. The pH of the BSA solution was adjusted with NaOH and HCl solutions. After this process, the fabrics were rinsed with water to remove the BSA excess. The modified BSA-PES textiles were then coated with RGO following the procedure shown in Section 2.4. Fig. 9 shows the electrical characterization by EIS of the PES-BSA-RGO fabrics. The values of impedance modulus obtained were 73 Ω, 356 Ω, 323 Ω, for pH 7, 4 and 10, respectively. This indicates that the optimal pH to coat the fabrics with RGO is neutral pH. With the plasma treatment, a BSA coating and one RGO coating, the value of |Z| achieved was similar to the value obtained for untreated PES coated with five RGO layers (73 Ω vs. 86.8 Ω, respectively). The plasma treatment and BSA coating increases the coating level of RGO on the fabric (as shown by SEM micrographs). A decrease in the electrical resistance of the conducting fabrics was also observed. To compare results, another PES fabric was coated with BSA and one RGO coating without applying the plasma treatment. The value of impedance modulus obtained was 306 Ω (value situated between 2 and 3 RGO coatings directly applied on PES).

3.5.Scanning electrochemical microscopy (SECM)

The electroactivity of the different RGO coated samples was tested by means of the SECM technique using approaching curves. To record these curves, the microelectrode was polarized at a potential (0 V) with which the oxidized form of the redox mediator (Ox) is reduced (Red) on the microelectrode surface at a diffusion controlled rate (Fig. 10). The measured current is defined as $i_\infty = 4 \cdot n \cdot F \cdot D \cdot C \cdot a$, where n is the number of electrons, F is the Faraday constant, D is the diffusion coefficient, C is the bulk concentration of the redox mediator, and a is the radius of the microelectrode tip. In

approaching curves, the normalized current registered at the microelectrode (I) is represented vs. the normalized distance (L). The normalized current is defined as follows: $I = i/i_{\infty}$ where "i" is the current measured at the UME tip and i_{∞} is the diffusion current defined above. The normalized current depends on RG (RG=Rg/a, where Rg is the radius of the insulating glass surrounding the Pt tip of radius "a") and the normalized distance L; where L=d/a (d is the microelectrode-substrate separation). The RG of the microelectrode used in this work was $RG \geq 20$.

Various situations can arise depending on the electroactivity of the substrates and the distance between the microelectrode and the substrate:

- When the microelectrode is sufficiently far from the substrate, the measured current corresponds to the diffusion current (i_{∞}).
- When the substrate is non-conductive, as the microelectrode approaches the substrate there is a hindrance to the diffusion of Ox species. The surface of the fabric is unable to regenerate (oxidize) the reduced form of the redox mediator (Red), hence there is a decrease in the reduction current on the surface of the microelectrode, $i<i_{\infty}$. This situation is known as negative feedback [50].
- Conversely, if the substrate is conductive, when the microelectrode approaches the surface, there is an increase of the oxidized redox species flux (Ox) since the surface potential is able to regenerate (oxidize) the redox mediator. This causes an increase in the current measured at the microelectrode, $i>i_{\infty}$. This case is known as positive feedback [50].

Experimental data was compared with theoretical approaching curves for positive and negative feedback models, according to equations 1 and 2. According to Rajendran *et al*. [51], Pade's approximation gives a close and simple equation with less relative error for all distances and valid for RG > 10. The approximate formula of the steady-state

normalized current assuming positive feedback for finite conductive substrate together with finite insulating glass thickness is:

$$I_T{}^{C} = \left[\frac{1 + 1.5647/L + 1.316855/L^2 + 0.4919707/L^3}{1 + 1.1234/L + 0.626395/L^2} \right] \quad (1)$$

The expression for the normalized current (assuming negative feedback) was based on the equation obtained by Bard *et al.*, for a RG=20 and L range 0.4-20 [52]:

$$I_T{}^{INS} = \left[\frac{1}{0.3554 + 2.0259/L + 0.62832 \times \exp\left(-2.55622/L\right)} \right] \quad (2)$$

Fig. 11 shows the approaching curves obtained by SECM for the different samples analyzed. The sample of PES-1G shows a slight negative feedback (there is a decrease in the normalized current as the microelectrode approaches the surface of the fabrics). The fabric is not completely coated with RGO and there are also zones that are not coated, but the sample behaves mainly as a non-electroactive material. The zones not coated prevailed over coated zones and negative feedback was obtained, although a pure negative feedback model was not achieved for this reason. When the number of RGO layers increased there was a better coverage of the surface of the fabric and positive feedback was obtained on the whole surface of the fabrics. Significant differences were not observed between 3, 5 and 10 RGO coatings, since similar values of feedback were achieved. In the SECM technique only the superficial coverage of the fabric has an effect on the electrochemical response obtained. In addition, the interconnection between the different RGO sheets or fibers has no effect; in this case the substrate is not polarized and operates at open circuit potential. On the other hand, in the conductivity measurements by EIS, it is this interconnection that provides the conductive pathways that allow the electrical flow.

When the PES fabric was treated with plasma and coated with BSA and one RGO coating, the fabric presented positive feedback across the whole surface. This indicates that the plasma and BSA coating improves the uniformity of the coating; and with only one RGO layer, a complete coverage of the surface of the fabric was achieved. The creation of functional groups by plasma and the posterior conversion of these negative groups to positive groups by BSA helps to improve the uniformity of the coating. The electroactivity obtained in this case was lower than the sample of PES coated with three RGO layers. This could be due to the presence of more RGO aggregates (electroactive) on the surface of the PES-3G sample.

3.6. Rubbing fastness tests

Rubbing fastness tests were performed in order to test the mechanical resistance of the RGO coatings against abrasion and to see whether there was an improvement in the mechanical resistance with the plasma and BSA treatment. The samples in this case were analyzed with FESEM and no extra coating was applied on the samples. The RGO coating served as conductive material. Taking advantage of this situation, the zones where the coating was removed could be easily identified as whiter zones due to the accumulation of electrons in non-conductive zones. Fig. 12-a, b show the FESEM micrographs for the sample of PES-plasma-BSA-1G prior to performing the rubbing fastness test. All the fibers were coated with RGO and the presence of RGO aggregates could also be observed (Fig. 12-b). When the rubbing test was performed whiter zones could be observed, which indicated the removal of the RGO coating in these zones (Fig. 12-c, d). The RGO aggregates were also removed from the surface of the fibers due to friction (as can be seen in Fig. 12-d). However, the degradation of the coating was not very high when compared to the PES-5G sample after performing the rubbing fastness

test (Fig. 12-e, f). In this case, the appearance of whiter zones due to the removal of the RGO coating was evident and extensive (Fig. 12-e). The degradation of the coating could also be observed with higher magnification (Fig. 12-f), the delamination of the RGO coating could be easily observed. The plasma and BSA treatment improves the adhesion of the RGO layers due to an improvement in the interaction forces between the fibers and coating. The influence of the chemical modification was observed with the fabrics obtained after plasma/BSA treatment. The comparison between the resistance values of the PES-plasma-BSA-1G fabric and the PES-1G fabric showed a value of |Z| of 73 Ω and 20967 kΩ, respectively. This represents a 287,000-fold improvement due to the chemical modification produced with plasma and BSA.

However, the physical modification (created mainly by increased roughness) that enabled an increase in the contact area between PES and RGO seemed to have less influence than the chemical modification. The physical modification influence was observed after chemically reducing a plasma treated fabric in order to eliminate the functional groups that did not allow the assembly of GO. The value of resistance obtained for the PES-plasma-reduced-1G fabric was 460 kΩ vs. 21000 kΩ for the untreated plasma PES-1G fabric, which was a 46-fold improvement.

Clearly, the chemical modification prevails over the physical modification in enhancing the adhesion and uniformity of the coating.

Electrical measurements showed in both cases an increase in the resistance of the fabrics of 7.5 % and 11 % for PES-5G and PES-plasma-BSA-1G, respectively. There was little difference between the sample treated with plasma and BSA and the untreated sample. The explanation for this fact is that the degradation is produced on the uppermost part of the fibers. The other parts of the fibers are still coated with RGO and allow electrical conduction [30].

The fabrics obtained could be employed as antistatic materials [21, 22] and also as support materials for depositing other materials such as nanoparticles:

- Pt nanoparticles for electrocatalysis to exploit the high surface area of the RGO and fabric with application for fuel cells [53, 54].
- Ti nanoparticles for photocatalysis. Self-cleaning textiles have been reported in the bibliography [55]. The combination of TiO_2 and graphene derivatives enhances photocatalytical activity due to an increased recombination time between electron and holes [56, 57]. The combination of TiO_2 and graphene derivatives has not been applied on fabrics to the best of our knowledge. In addition it could be a good way to support the photocatalyst.

More work is in progress to combine RGO fabrics with Pt and TiO_2 nanoparticles and study performance for electrochemical and photocatalytic systems.

4. Conclusions

A plasma technique has been used to increase the surface adhesion of reduced graphene oxide (RGO) on polyester (PES) fabrics. Polyester fabrics were treated with an atmospheric plasma (dielectric barrier discharge) with different plasma dosages. The surface energy (measured by contact angle measurements) and the surface roughness (measured by atomic force microscopy or AFM) increased with the plasma dosage applied until there was a stabilization with a plasma dosage of 3000 $W \cdot min \cdot m^{-2}$. Higher plasma dosages only produced an increase in energy consumption.

The plasma treatment generated negative charges on the surface of PES, hence the self-assembly of GO on plasma treated PES fabrics was impossible under these conditions since GO also presents negative charges. For this reason, an intermediate coating

between GO and PES was employed to generate positive charges on the surface of the fabric and allow the assembly of GO. The coating used for this purpose was the protein bovine serum albumin (BSA).

Scanning electron microscopy (SEM) showed the formation of RGO coatings on the surface of PES fibers. The plasma treatment and BSA coating produced an increase in the coating level on the fabrics when compared with untreated fabrics. AFM also showed the deposition of RGO on the surface of plasma treated fabrics.

The electrical resistance of the fabrics was measured using electrochemical impedance spectroscopy (EIS). The treatment of the fabrics with plasma and BSA produced a decrease in the resistance of the fabrics due to an increase in the coating level of the fabrics. With only one RGO coating, values of resistance similar to the untreated sample of PES coated with five RGO coatings were obtained. The plasma treatment decreased the number of coatings needed to achieve similar values of electrical resistance. This enables a reduced processing time and also a saving in chemical products and water. This would justify the application of the plasma/BSA treatment.

The electroactivity of conductive fabrics was measured with scanning electrochemical microscopy (SECM) using approaching curves. The treatment with plasma and BSA improved the electroactivity of the fabrics with the application of fewer RGO coatings due to an improved surface coverage.

Mechanical resistance of the coatings was tested by means of rubbing fastness tests. The plasma treatment and BSA coating increased the adhesion of RGO to the surface of PES fibers as FESEM micrographs have shown.

Acknowledgements

The authors wish to thank to the Spanish Ministry of Science and Innovation (contract CTM2011-23583) for their financial support. J. Molina is grateful to the Department of Education, Training and Work (Generalitat Valenciana) for the Programa VALi+D Postdoctoral Fellowship. The Electron Microscopy Service of the UPV (Universitat Politècnica de València) is gratefully acknowledged for helping with FESEM and AFM characterization.

References

[1] A.R. Horrocks, B.K. Kandola, P.J. Davies, S. Zhang, S.A. Padbury, Developments in flame retardant textiles – a review, Polym. Degrad. Stabil. 88 (2005) 3–12.

[2] M. Yu, Z. Wang, H. Liu, S. Xie, J. Wu, H. Jiang, J. Zhang, L. Li, J. Li, Laundering durability of photocatalyzed self-cleaning cotton fabric with TiO_2 nanoparticles covalently immobilized, ACS Appl. Mater. Interfaces 5 (2013) 3697–3703.

[3] Y. Shin, D. Yoo, K. Son, Development of thermoregulating textile materials with microencapsulated phase change materials (PCM). II. Preparation and application of PCM microcapsules, J. Appl. Polym. Sci. 96 (2005) 2005–2010.

[4] R.F. Service, Electronic textiles charge ahead, Science 301 (2003) 909–911.

[5] J.W. Lee, T. Mayer-Gall, K. Opwis, C.E. Song, J.S. Gutmann, B. List, Organotextile catalysis, Science 341 (2013) 1225–1229.

[6] S. Coyle, Y. Wu, K.-T. Lau, D. De Rossi, G. Wallace, D. Diamond, Smart nanotextiles: A review of materials and applications, MRS Bulletin 32 (2007) 434–442.

[7] E. Romero, J. Molina, A.I. del Río, J. Bonastre, F. Cases, Synthesis of PPy/$PW_{12}O_{40}^{3-}$ organic-inorganic hybrid material on polyester yarns and subsequent weaving to obtain conductive fabrics, Text. Res. J. 81 (2011) 1427–1437.

[8] A. Bhattacharyya, M. Joshi, Development of polyurethane based conducting nanocomposite fibers via twin screw extrusion, Fiber. Polym. 12 (2011) 734–740.

[9] A. Kaynak, S.S. Najar, R.C. Foitzik, Conducting nylon, cotton and wool yarns by continuous vapor polymerization of pyrrole, Synth. Met. 158 (2008) 1–5.

[10] J. Molina, J. Fernández, A.I. del Río, R. Lapuente, J. Bonastre, F. Cases, Stability of conducting polyester/polypyrrole fabrics in different pH solutions. Chemical and electrochemical characterization, Polym. Degrad. Stabil. 95 (2010) 2574–2583.

[11] J. Molina, J. Fernández, A.I. del Río, J. Bonastre, F. Cases, Chemical, electrical and electrochemical characterization of hybrid organic/inorganic polypyrrole/$PW_{12}O_{40}^{3-}$ coating deposited on polyester fabrics, Appl. Surf. Sci. 257 (2011) 10056–10064.

[12] K.S. Novoselov, A.K. Geim, S.V. Morozov, D. Jiang, Y. Zhang, S.V. Dubonos, I.V. Grigorieva, A.A. Firsov, Electric field effect in atomically thin carbon films, Science 306 (2004) 666−669.

[13] K.S. Novoselov, V.I. Fal'ko, L. Colombo, P.R. Gellert, M.G. Schwab, K. Kim, A roadmap for graphene, Nature 490 (2012) 192−200.

[14] F. Bonaccorso, Z. Sun, T. Hasan, A.C. Ferrari, Graphene photonics and optoelectronics, Nat. Photonics 4 (2010) 611−622.

[15] A.H. Castro Neto, F. Guinea, N.M.R. Peres, K.S. Novoselov, A.K. Geim, The electronic properties of graphene, Rev. Mod. Phys. 81 (2009) 109−162.

[16] H.B. Heersche, P. Jarillo-Herrero, J.B. Oostinga, L.M.K. Vandersypen, A.F. Morpurgo, Bipolar supercurrent in graphene, Nature 446 (2007) 56−59.

[17] A.N. Grigorenko, M. Polini, K.S. Novoselov, Graphene plasmonics, Nat. Photonics 6 (2012) 749−758.

[18] C. Soldano, A. Mahmood, E. Dujardin, Production, properties and potential of graphene, Carbon 48 (2010) 2127−2150.

[19] V. Singh, D. Joung, L. Zhai, S. Das, S.I. Khondaker, S. Seal, Graphene based materials: Past, present and future, Prog. Mater. Sci. 56 (2011) 1178–1271.

[20] S. Park, R.S. Ruoff, Chemical methods for the production of graphenes, Nat. Nanotechnol. 4 (2009) 217−224.

[21] J. Molina, J. Fernández, J.C. Inés, A.I. del Río, J. Bonastre, F. Cases, Electrochemical characterization of reduced graphene oxide-coated polyester fabrics, Electrochim. Acta 93 (2013) 44–52.

[22] J. Molina, J. Fernández, A.I. del Río, J. Bonastre, F. Cases, Chemical and electrochemical study of fabrics coated with reduced graphene oxide, Appl. Surf. Sci. 279 (2013) 46–54.

[23] M. Shateri-Khalilabad, M.E. Yazdanshenas, Fabricating electroconductive cotton textiles using graphene, Carbohyd. Polym. 96 (2013) 190–195.

[24] M. Shateri-Khalilabad, M.E. Yazdanshenas, Preparation of superhydrophobic electroconductive graphene-coated cotton cellulose, Cellulose 20 (2013) 963–972.

[25] Y.J. Yun, W.G. Hong, W.-J. Kim, Y. Jun, B.H. Kim, A novel method for applying reduced graphene oxide directly to electronic textiles from yarns to fabrics, Adv. Mater. 25 (2013) 5701–5705.

[26] B. Fugetsu, E. Sano, H. Yu, K. Mori, T. Tanaka, Graphene oxide as dyestuffs for the creation of electrically conductive fabrics, Carbon 48 (2010) 3340–3345.

[27] W. Gu, Y. Zhao, Graphene modified cotton textiles, Adv. Mat. Res. 331 (2011) 93−96.

[28] Y.-L. Huang, A. Baji, H.-W. Tien, Y.-K. Yang, S.-Y. Yang, C.-C.M. Ma, H.-Y. Liu, Y.-W. Mai, N.-H. Wang, Self-assembly of graphene onto electrospun polyamide 66 nanofibers as transparent conductive thin films, Nanotechnology 22 (2011) 475603.

[29] G. Yu, L. Hu, M. Vosgueritchian, H. Wang, X. Xie, J.R. McDonough, X. Cui, Y. Cui, Z. Bao, Solution-processed graphene/MnO_2 nanostructured textiles for high-performance electrochemical capacitors, Nano Lett. 11 (2011) 2905–2911.

[30] J. Molina, F. R. Oliveira, A. P. Souto, M. F. Esteves, J. Bonastre, F. Cases, Enhanced adhesion of polypyrrole/$PW_{12}O_{40}^{3-}$ hybrid coatings on polyester fabrics, J. Appl. Polym. Sci. 129 (2013) 422–433.

[31] F. Leroux, C. Campagne, A. Perwuelz, L. Gengembre, Atmospheric air plasma treatment of polyester textile materials. Textile structure influence on surface oxidation and silicon resin adhesion, Surf. Coat. Technol. 203 (2009) 3178–3183.

[32] C.W. Kan, K. Chan, C.W.M. Yuen, M.H.J. Miao, The effect of low temperature plasma on chrome dyeing of wool fibres, J. Mater. Process. Technol. 82 (1998) 122–126.

[33] S. Garg, C. Hurren, A. Kaynak, Improvement of adhesion of conductive polypyrrole coating on wool and polyester fabrics using atmospheric plasma treatment, Synth. Met. 157 (2007) 41–47.

[34] Complete textile glossary, available from: http://www.celaneseacetate.com/textile_glossary_filament_acetate.pdf, 2001. Last accessed 15th November 2012.

[35] N. Carneiro, A.P. Souto, F. Forster, E. Prinz, Patent in internationalization phase (2004)/ patent number PCT/PT2004/000008,2004.

[36] F.R. Oliveira, M. Fernandes, N. Carneiro, A.P. Souto, Functionalization of wool fabric with phase-change materials microcapsules after plasma surface modification, J. Appl. Polym. Sci. 128 (2013) 2638–2647.

[37] C. Riccardi, R. Barni, E. Selli, G. Mazzone, M.R. Massafra, B. Marcandallic, G. Poletti, Surface modification of poly(ethylene terephthalate) fibers induced by radio frequency air plasma treatment, Appl. Surf. Sci. 211 (2003) 386–397.

[38] M.R. Sanchis, V. Blanes, M. Blanes, D. Garcia, R. Balart, Surface modification of low density polyethylene (LDPE) film by low pressure O_2 plasma treatment, Eur. Polym. J. 42 (2006) 1558–1568.

[39] A. Zille, F.R. Oliveira, A.P. Souto, Plasma treatment in textile industry, Plasma Process. Polym. 2014, DOI: 10.1002/ppap.201400052.

[40] J. Yip, K. Chan, K.M. Sin, K.S. Lau, Study of physico-chemical surface treatments on dyeing properties of polyamides. Part 1: Effect of tetrafluoromethane low temperature plasma, Color. Technol. 118 (2002) 26–30.

[41] C. Jia, P. Chen, B. Li, Q. Wang, C. Lu, Q. Yu, Effects of twaron fiber surface treatment by air dielectric barrier discharge plasma on the interfacial adhesion in fiber reinforced composites, Surf. Coat. Technol. 204 (2010) 3668–3675.

[42] L.C.V. Wielen, M. Östenson, P. Gatenholm, A.J. Ragauskas, Surface modification of cellulosic fibers using dielectric-barrier discharge, Carbohyd. Polym. 65 (2006) 179–184.

[43] S. Stankovich, D.A. Dikin, G.H.B. Dommett, K.M. Kohlhaas, E.J. Zimney, E.A. Stach, R.D. Piner, S.T. Nguyen, R.S. Ruoff, Graphene-based composite materials, Nature 440 (2006) 282–286.

[44] D.R. Dreyer, S. Park, C.W. Bielawski, R.S. Ruoff, The chemistry of graphene oxide, Chem. Soc. Rev. 39 (2010) 228–240.

[45] D. Chen, H. Feng, J. Li, Graphene oxide: preparation, functionalization, and electrochemical applications, Chem. Rev. 112 (2012) 6027−6053.

[46] C. Vallés, J.D. Núñez, A.M. Benito, W.K. Maser, Flexible conductive graphene paper obtained by direct and gentle annealing of graphene oxide paper, Carbon 50 (2012) 835−844.

[47] L. Guo, C. Campagne, A. Perwuelz, F. Leroux, Zeta potential and surface physico-chemical properties of atmospheric air-plasma-treated polyester fabrics, Text. Res. J. 79 (2009) 1371–1377.

[48] D. Li, M.B. Müller, S. Gilje, R.B. Kaner, G.G. Wallace, Processable aqueous dispersions of graphene nanosheets, Nat. Nanotechnol. 3 (2008) 101–105.

[49] A. Michnik, K. Michalik, Z. Drzazga, Stability of bovine serum albumin at different pH, J. Therm. Anal. Calorim. 80 (2005) 399–406.

[50] P. Sun, F.O. Laforge, M.V. Mirkin, Scanning electrochemical microscopy in the 21st century, Phys. Chem. Chem. Phys. 9 (2007) 802–823.

[51] L. Rajendran, S.P. Ananthi, Analysis of positive feedback currents at the scanning electrochemical microscope, J. Electroanal. Chem. 561 (2004) 113–118.

[52] A.J. Bard, M.V. Mirkin, Scanning Electrochemical Microscopy, Marcel Dekker Inc., New York, 2001.

[53] J. Molina, J. Fernández, A.I. del Río, J. Bonastre, F. Cases, Synthesis of Pt nanoparticles on electrochemically reduced graphene oxide by potentiostatic and alternate current methods, Mater. Charact. 89 (2014) 56–68.

[54] H. Huang, H. Chen, D. Sun, X. Wang, Graphene nanoplate-Pt composite as a high performance electrocatalyst for direct methanol fuel cells, J Power Sources 204 (2012) 46–52.

[55] N.M. Bedford, A.J. Steckl, Photocatalytic self-cleaning textile fibers by coaxial electrospinning, ACS Appl. Mater. Interfaces 2 (2010) 2448–2455.

[56] X. Cao, G. Tian, Y. Chen, J. Zhou, W. Zhou, C. Tiana, H. Fu, Hierarchical composites of TiO2 nanowire arrays on reduced graphene oxide nanosheets with enhanced photocatalytic hydrogen evolution performance, J. Mater. Chem. A 2 (2014) 4366–4374.

[57] Y. Zhao, D. Zhao, C. Chen, X. Wang, Enhanced photo-reduction and removal of Cr(VI) on reduced grapheme oxide decorated with TiO_2 nanoparticles, J. Colloid Interf. Sci. 405 (2013) 211–217.

Figure captions

Fig. 1. Dynamic contact angle measurements for untreated polyester fabrics and plasma treated polyester fabric with a dosage of 500 $W \cdot min \cdot m^{-2}$.

Fig. 2. AFM 3D representations of polyester treated with different plasma dosages: (a) 0 $W \cdot min \cdot m^{-2}$ (b) 500 $W \cdot min \cdot m^{-2}$, (c) 3000 $W \cdot min \cdot m^{-2}$, (d) 7500 $W \cdot min \cdot m^{-2}$.

Fig. 3. AFM 2D representation of polyester treated with different plasma dosages: (a) 0 $W \cdot min \cdot m^{-2}$ (b) 500 $W \cdot min \cdot m^{-2}$, (c) 3000 $W \cdot min \cdot m^{-2}$, (d) 7500 $W \cdot min \cdot m^{-2}$. (e) Section roughness profiles of the 2D representations shown.

Fig. 4. SEM micrographs of (a) PES-1G (×1000), (b) PES-3G (×1000), (c) PES-5G (×1000) and (d) PES-10G (×1000).

Fig. 5. SEM micrographs of PES treated with plasma 3000 $W \cdot min \cdot m^{-2}$ and coated with BSA and RGO (a) (×2000), (b) (×3500).

Fig. 6. AFM analysis of polyester treated with plasma (3000 $W \cdot min \cdot m^{-2}$) and coated with BSA and one layer of RGO. (a) 3D representation, (b) 2D representation, (c) section roughness profile shown in (b).

Fig. 7. Bode plots for PES coated with a different number of RGO coatings (1, 3, 5 and 10). Samples of PES and PES-GO are also shown as reference. Samples located between two metallic conductors. Frequency range from 10^5 Hz to 10^{-2} Hz.

Fig. 8. Bode plots for PES treated with different plasma dosages (500, 3000, and 7500 $W \cdot min \cdot m^{-2}$) and coated with one layer of RGO. PES treated with plasma (3000 $W \cdot min \cdot m^{-2}$) and reduced chemically and coated with one layer of RGO, and an untreated PES coated with one layer RGO are also shown for comparison. Samples located between two metallic conductors. Frequency range from 10^5 Hz to 10^{-2} Hz.

Fig. 9. Bode plots for PES treated with plasma (3000 $W \cdot min \cdot m^{-2}$) without RGO coating and PES treated with the plasma (3000 $W \cdot min \cdot m^{-2}$) and coated with BSA at different pH (4, 7, 10) and coated with one layer of RGO. Samples located between two metallic conductors. Frequency range from 10^5 Hz to 10^{-2} Hz.

Fig. 10. Cyclic voltammogram obtained with a 100 µm diameter Pt SECM-tip in $K_3Fe(CN)_6$ 0.01 M and 0.1 M KCl solution; scan rate 50 $mV \cdot s^{-1}$.

Fig. 11. Approaching curves for PES-1G, PES-3G, PES-5G, PES-10G, PES-plasma-BSA-1G (continuous lines), theoretical negative feedback model () and theoretical positive feedback model (Δ). Obtained with a 100 µm diameter Pt SECM-tip in $K_3Fe(CN)_6$ 0.01 M and 0.1 M KCl. The tip potential was 0 mV (vs. Ag/AgCl) and the approaching rate was 10 $\mu m \cdot s^{-1}$.

Fig. 12. FESEM micrographs of: a), b) PES-plasma-BSA-1G; c), d) PES-plasma-BSA-1G after rubbing fastness test; e), f) PES-5G after rubbing fastness test.

Table captions

Table 1. Conditions and plasma dosages applied to polyester fabrics.

Table 2. Values of contact angles (º) (water, glycerol and polyethylene glycol) and surface energy values ($mJ \cdot m^{-2}$) for PES treated with different plasma dosages.

Table 3. Values of impedance modulus |Z| obtained for the different fabrics.

Table 1

Table 1. Conditions and plasma dosages applied to polyester fabrics.

Sample	Velocity ($m \cdot min^{-1}$)	Power (W)	Nº passages	Dosage ($W \cdot min \cdot m^{-2}$)
1	0	0	0	0
2	4	1000	1	500
3	4	1000	3	1500
4	4	1000	6	3000
5	4	1000	9	4500
6	4	1000	12	6000
7	4	1000	15	7500

Table 2

Table 2. Values of contact angles (º) (water, glycerol and polyethylene glycol) and surface energy values ($mJ \cdot m^{-2}$) for PES treated with different plasma dosages.

Dosage ($W \cdot min \cdot m^{-2}$)	Contact angle water (°)	Contact angle glycerol (°)	Contact angle PEG (°)	Total surface energy ($mJ \cdot m^{-2}$)	Dispersive energy ($mJ \cdot m^{-2}$)	Polar energy ($mJ \cdot m^{-2}$)
0	130.5±6.3	143.2±6.6	51.0±4.0	10.50	10	0.50
500	42.7±7.6	119.3±2.0	40.0±3.1	67.03	0.84	66.19
1500	13.2±2.5	107.2±2.7	37.7±1.0	117.41	0.41	117.00
3000	5.0±4.1	108.3±3.6	36.8±1.1	124.63	0.22	124.41
4500	6.5±3.4	112.5±7.0	36.9±1.2	126.25	0	126.25
6000	6.9±5.9	113.1±2.6	34.9±1.5	123.01	0	123.01
7500	0.0±0.0	112.5±4.3	34.0±1.2	123.95	0	123.95

Table 3

Impedance modulus |Z| (Ω)				
PES/G				
PES-0G	**PES-1G**	**PES-3G**	**PES-5G**	**PES-10G**
$>10^{11}$	$2.1 \cdot 10^{7}$	145	87	9
PES/plasma treatment (3000 W·min·m^{-2})/1G				
$>10^{11}$				
PES/plasma treatment (3000 W·min·m^{-2})/chemical reduction/1G				
$4.6 \cdot 10^{5}$				
PES/plasma treatment (3000 W·min·m^{-2})/BSA/1G				
pH 4		**pH 7**		**pH 10**
356		73		323

Table 3. Values of impedance modulus |Z| obtained for the different fabrics.

Figure 1

Click here to download high resolution image

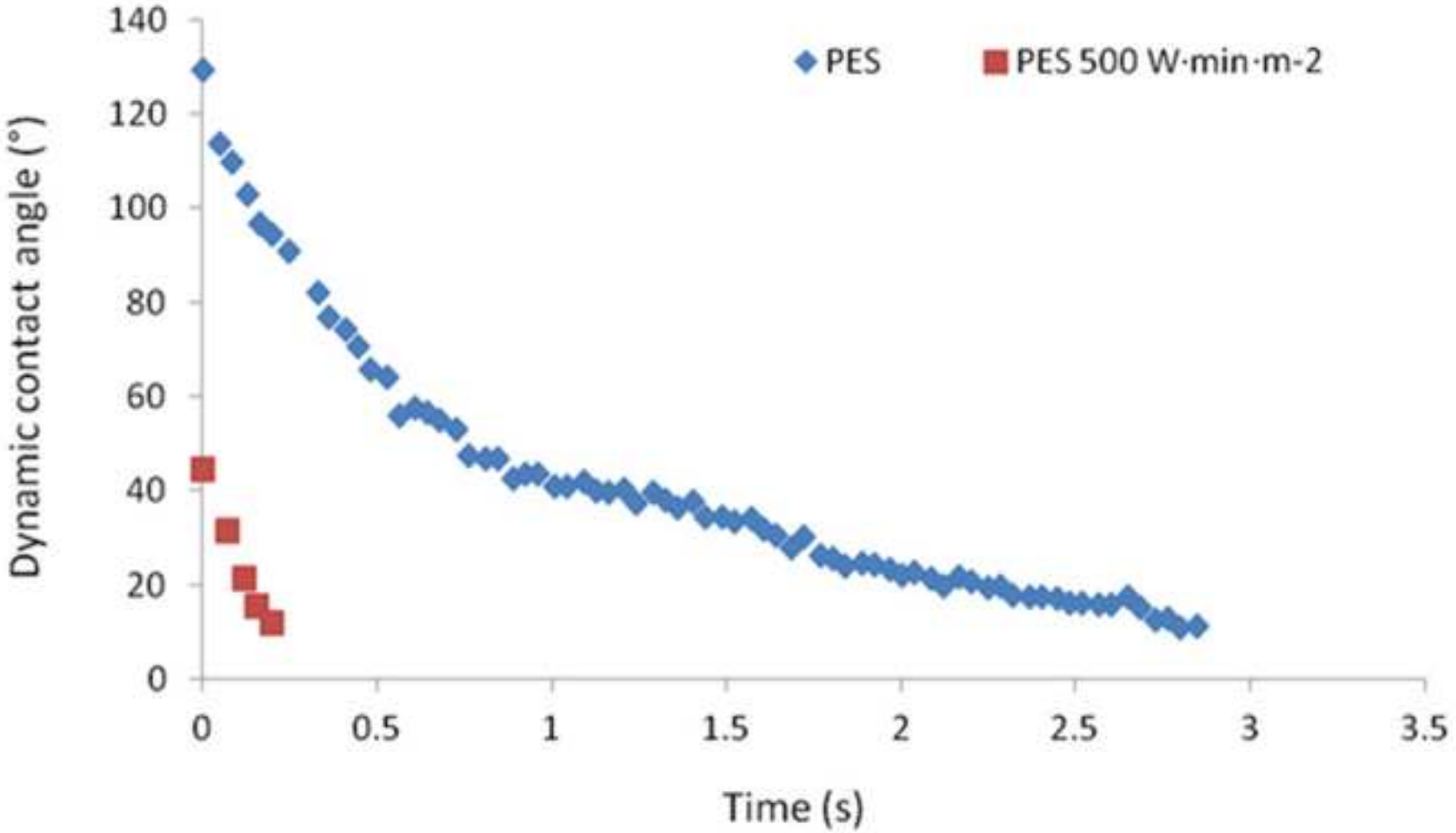

Figure 2

Click here to download high resolution image

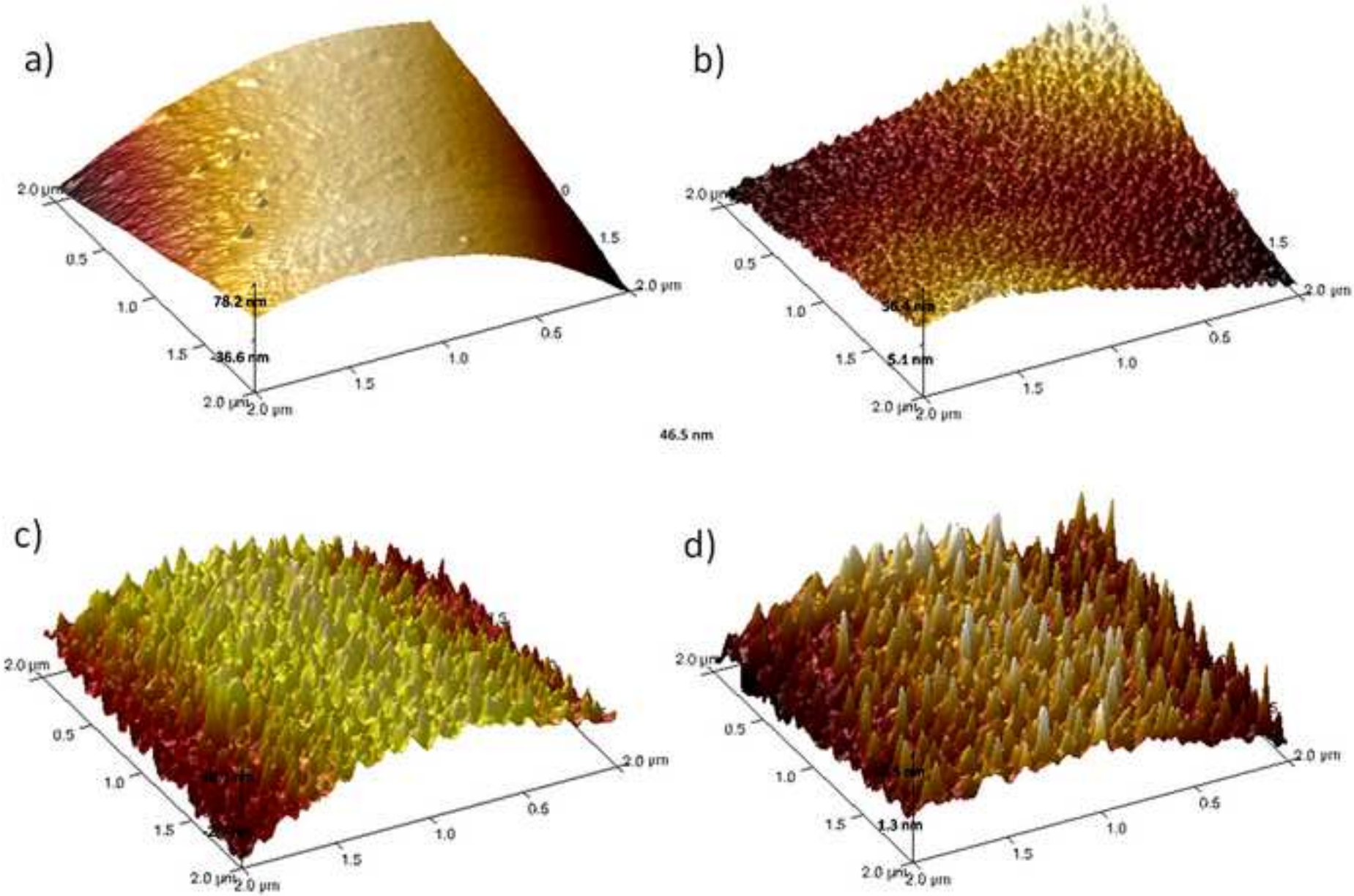

Figure 3

Click here to download high resolution image

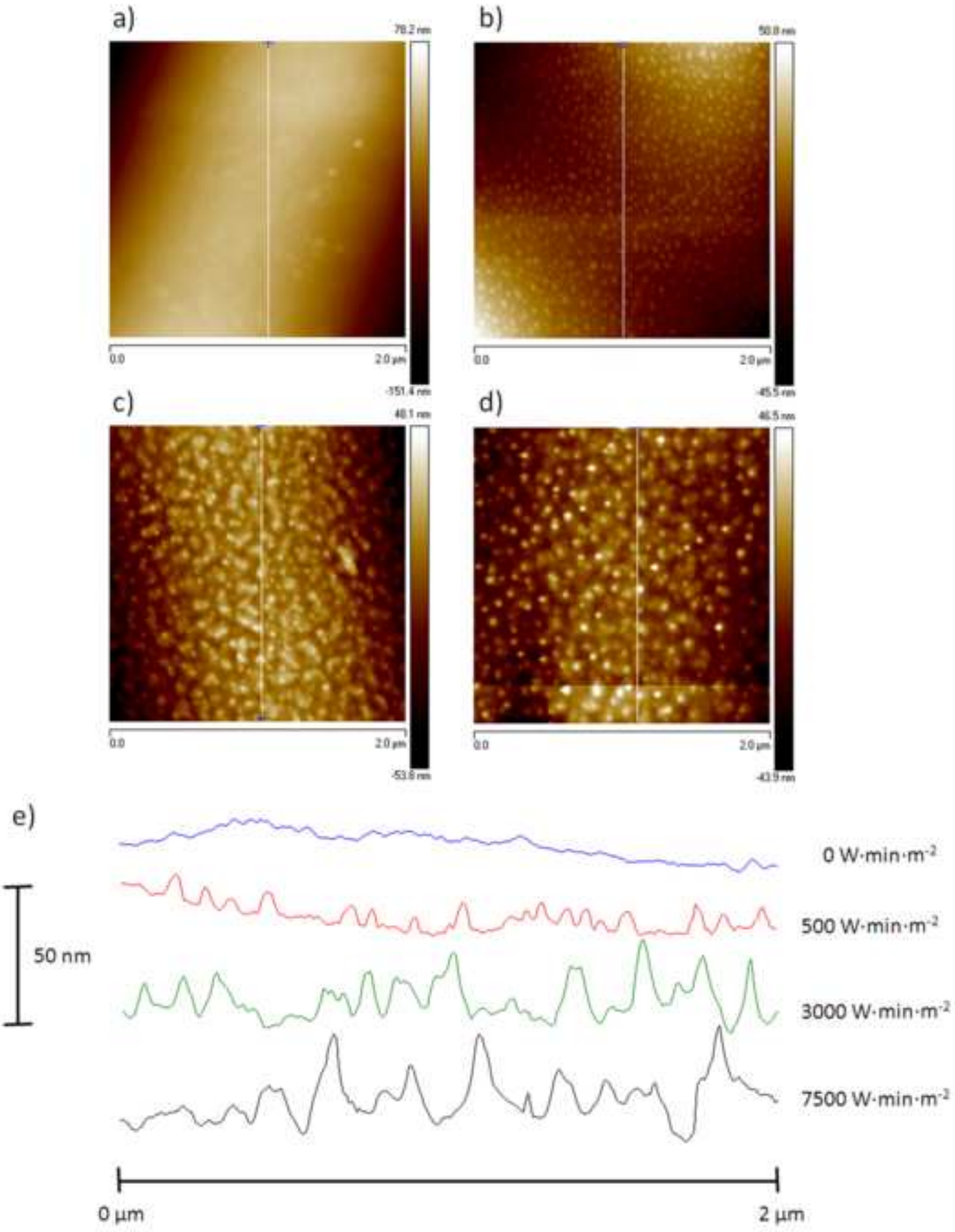

Figure 4

Click here to download high resolution image

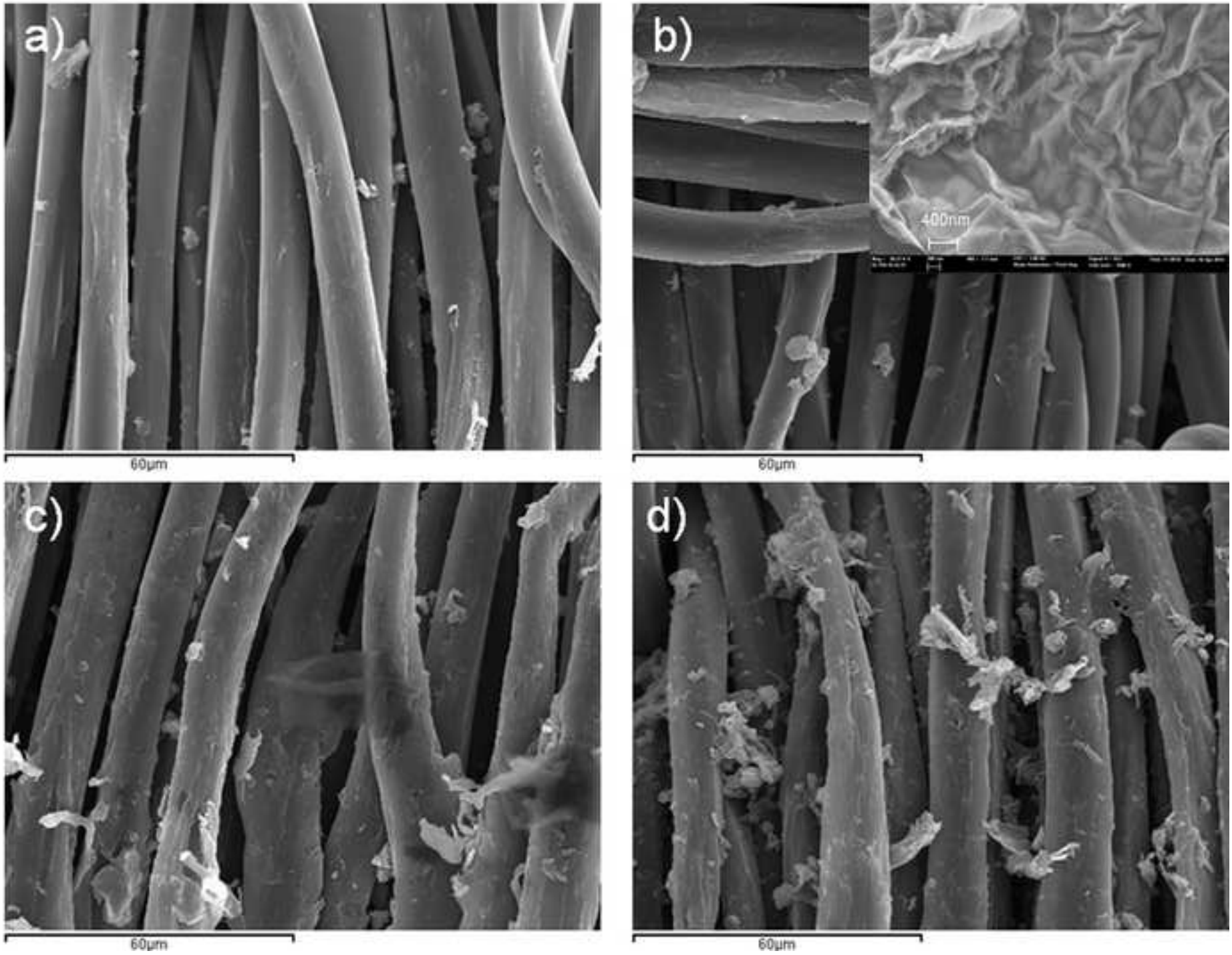

Figure 5

Click here to download high resolution image

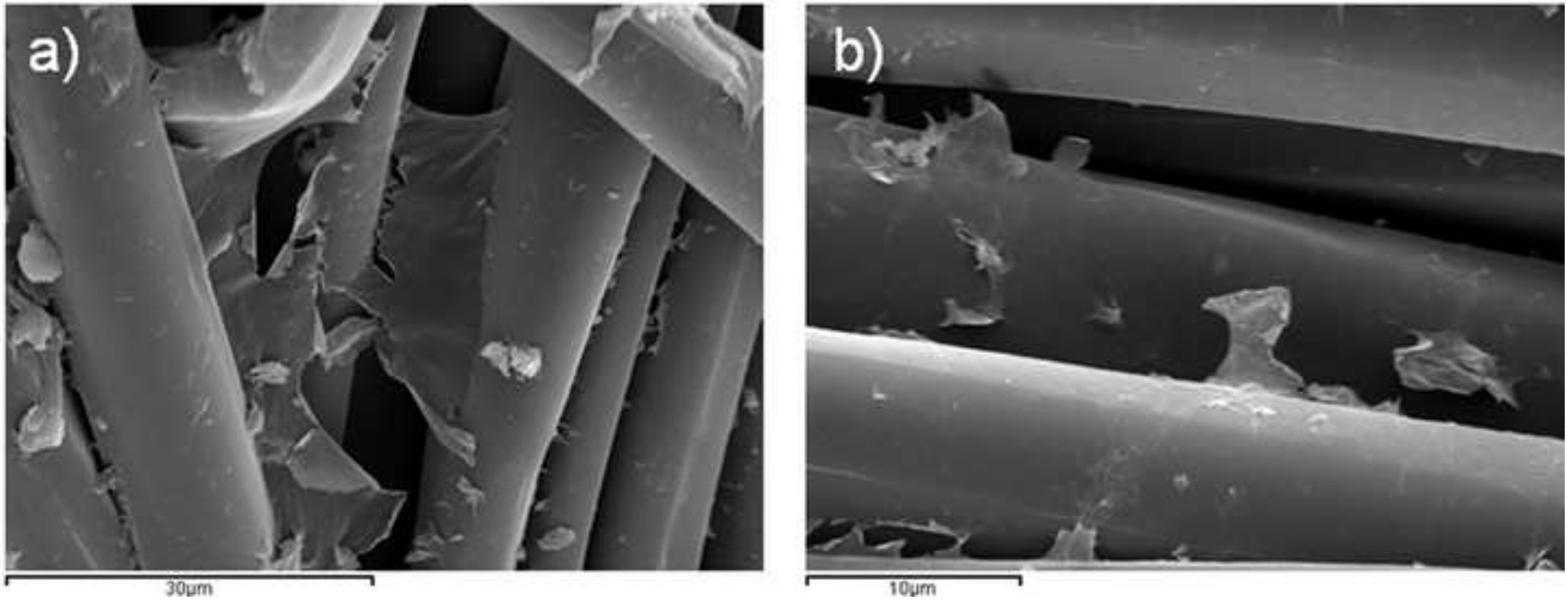

Figure 6

Click here to download high resolution image

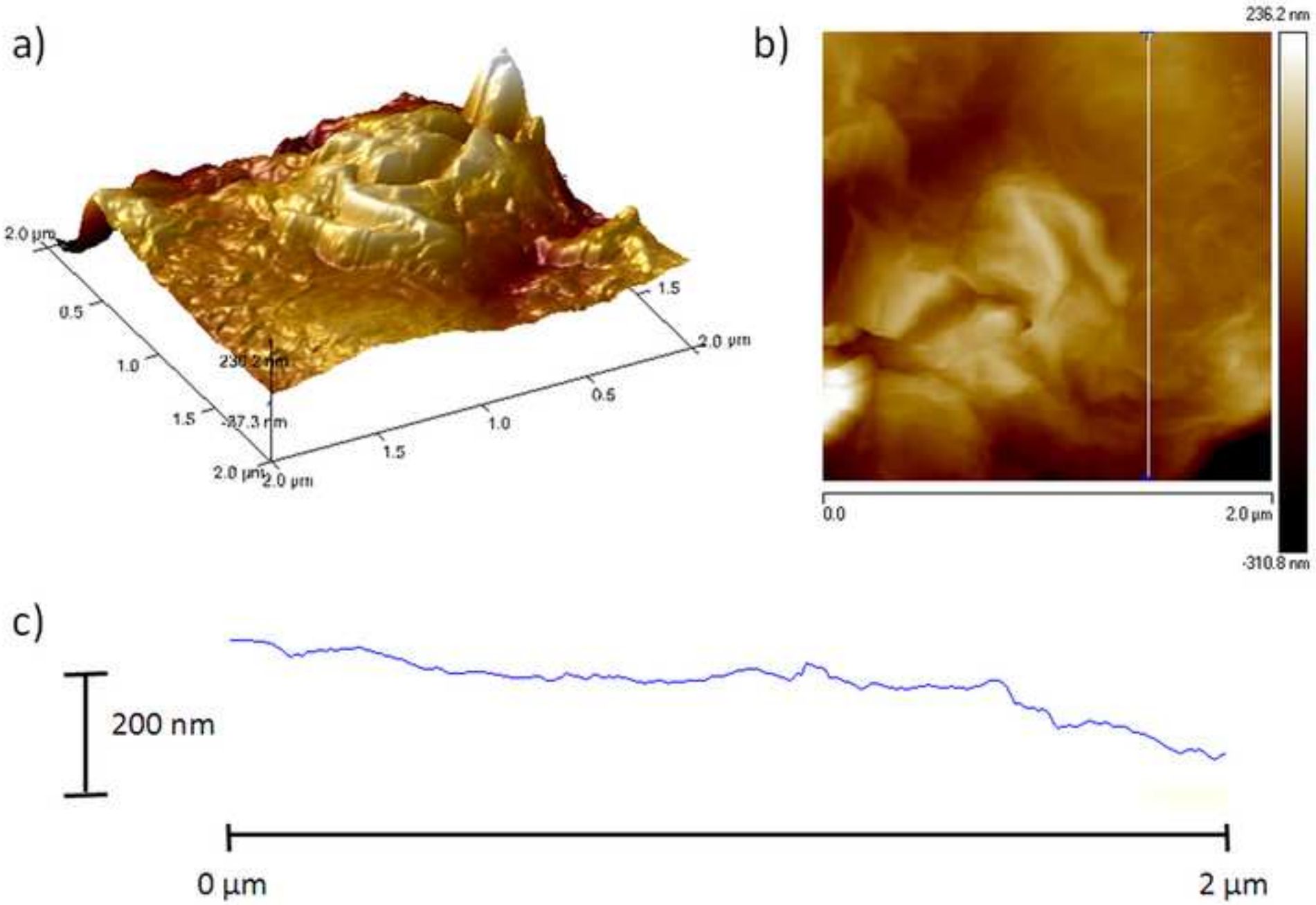

Figure 7
Click here to download high resolution image

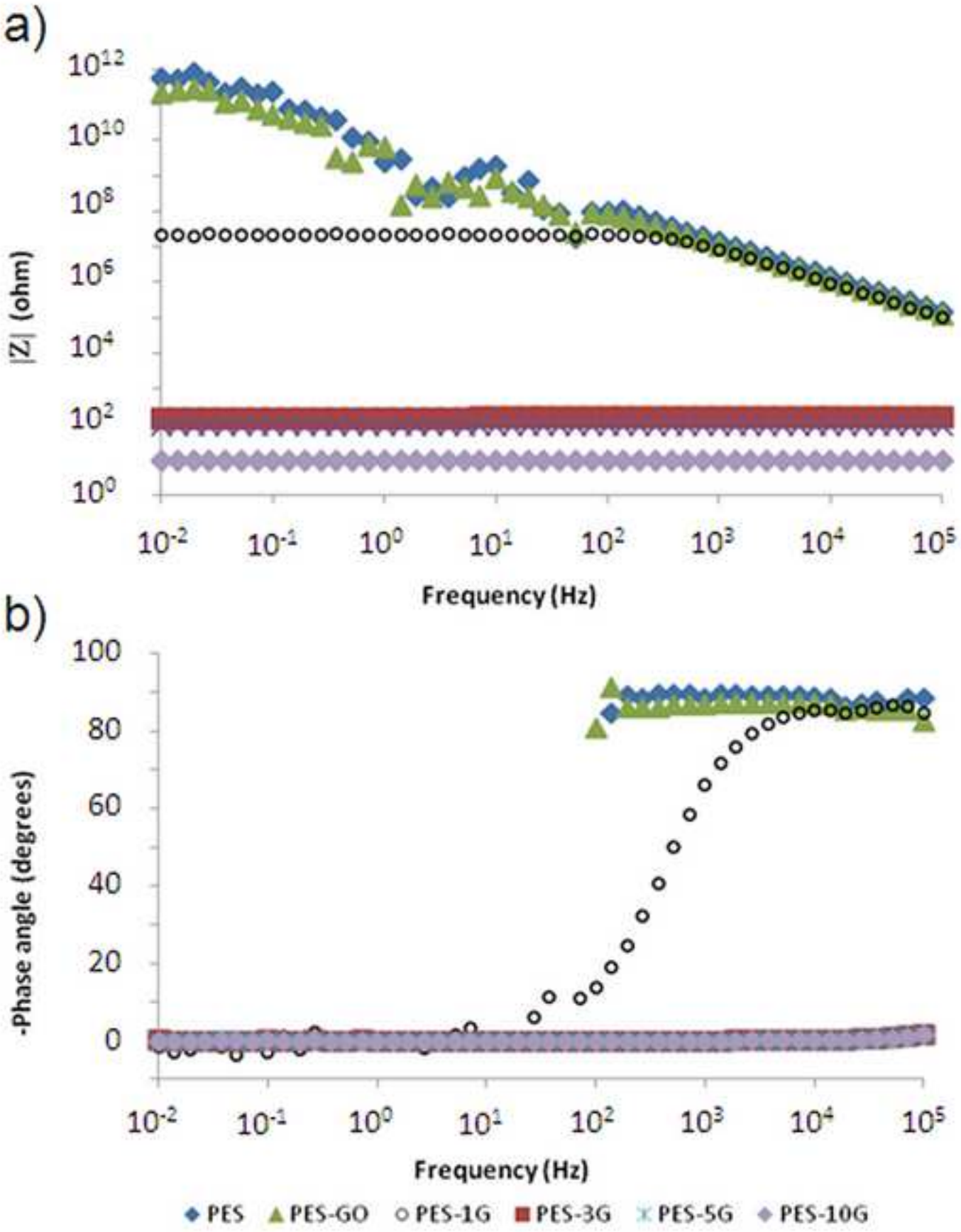

Figure 8

Click here to download high resolution image

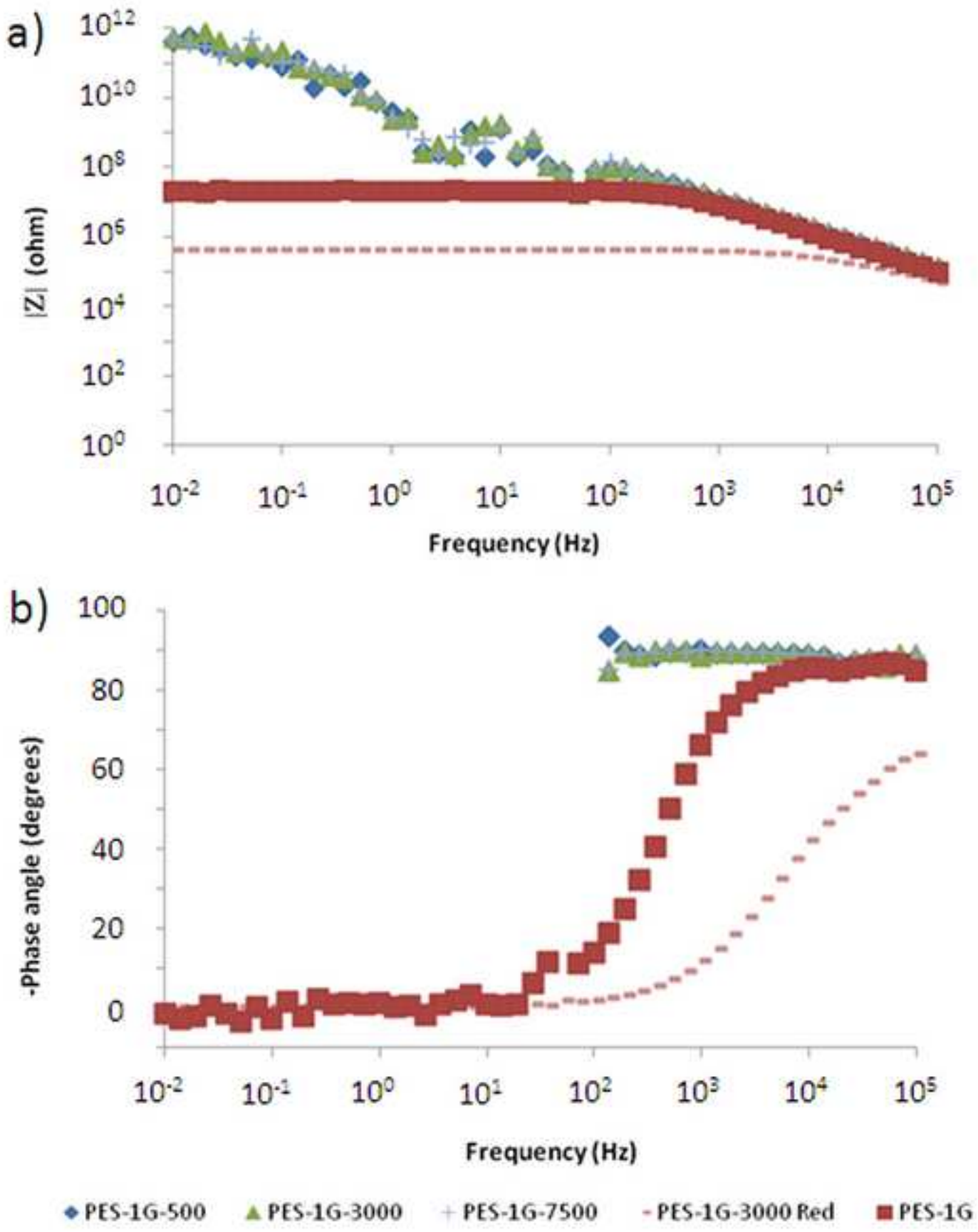

Figure 9
Click here to download high resolution image

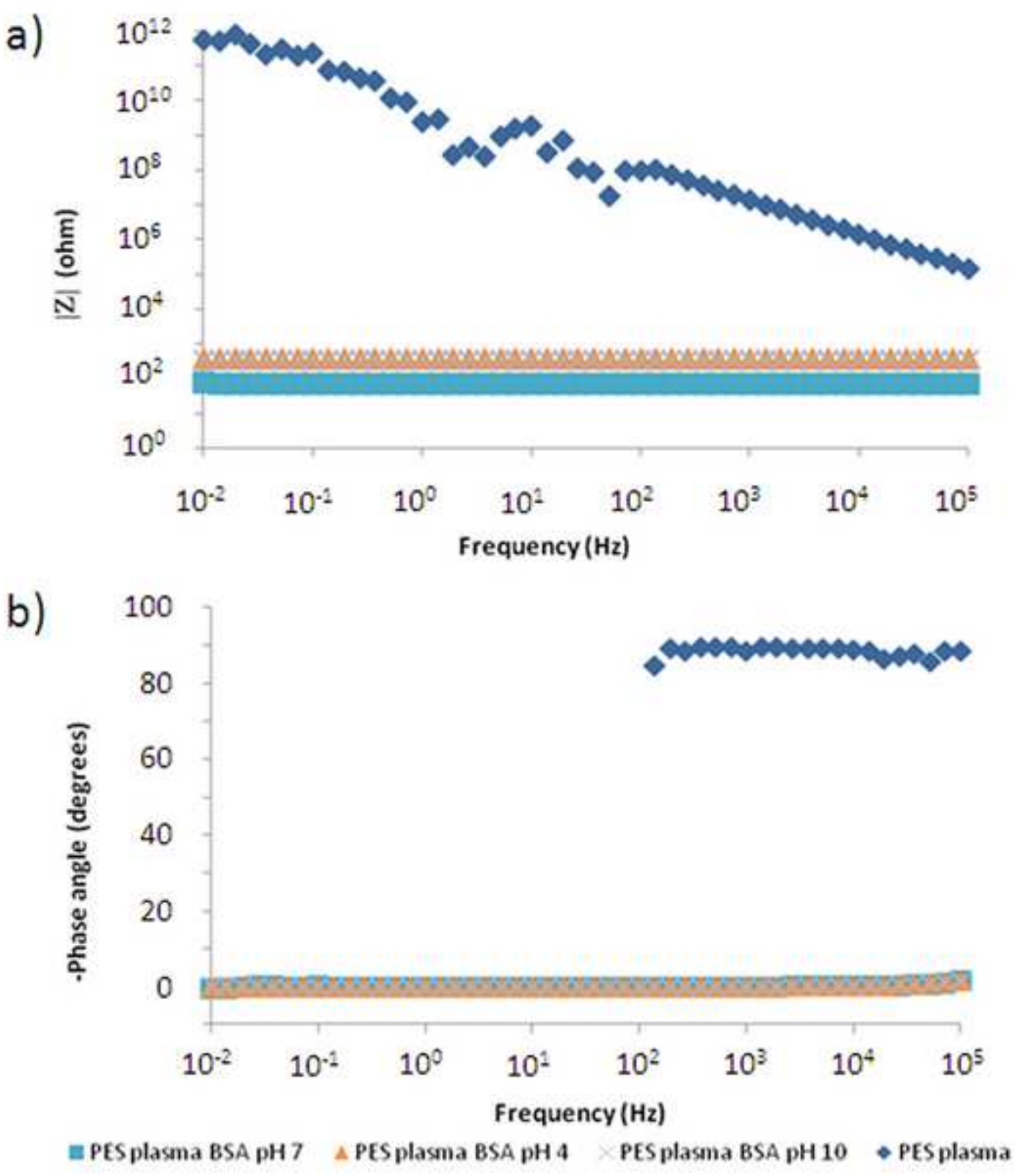

Figure 10

Click here to download high resolution image

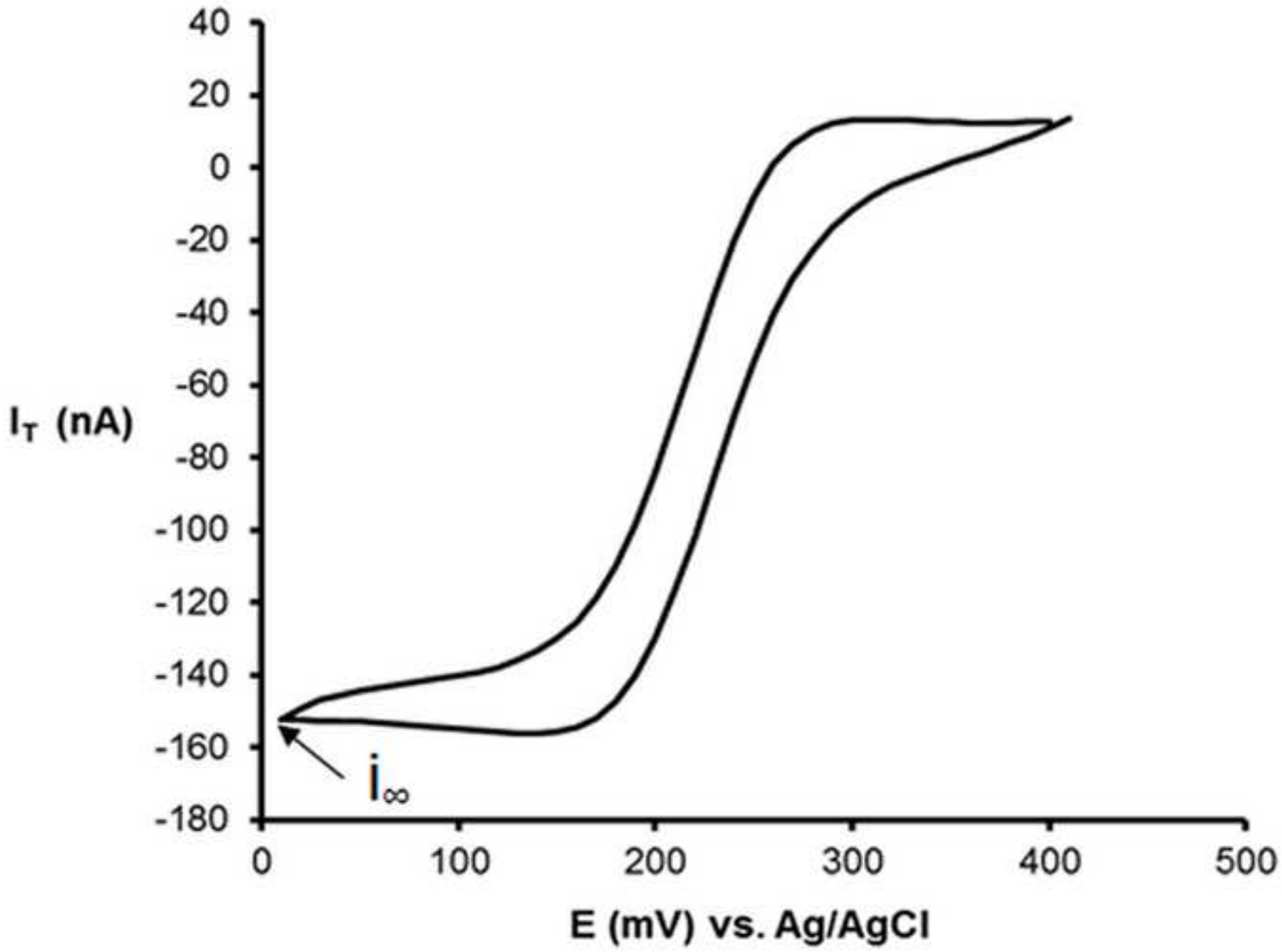

Figure 11

Click here to download high resolution image

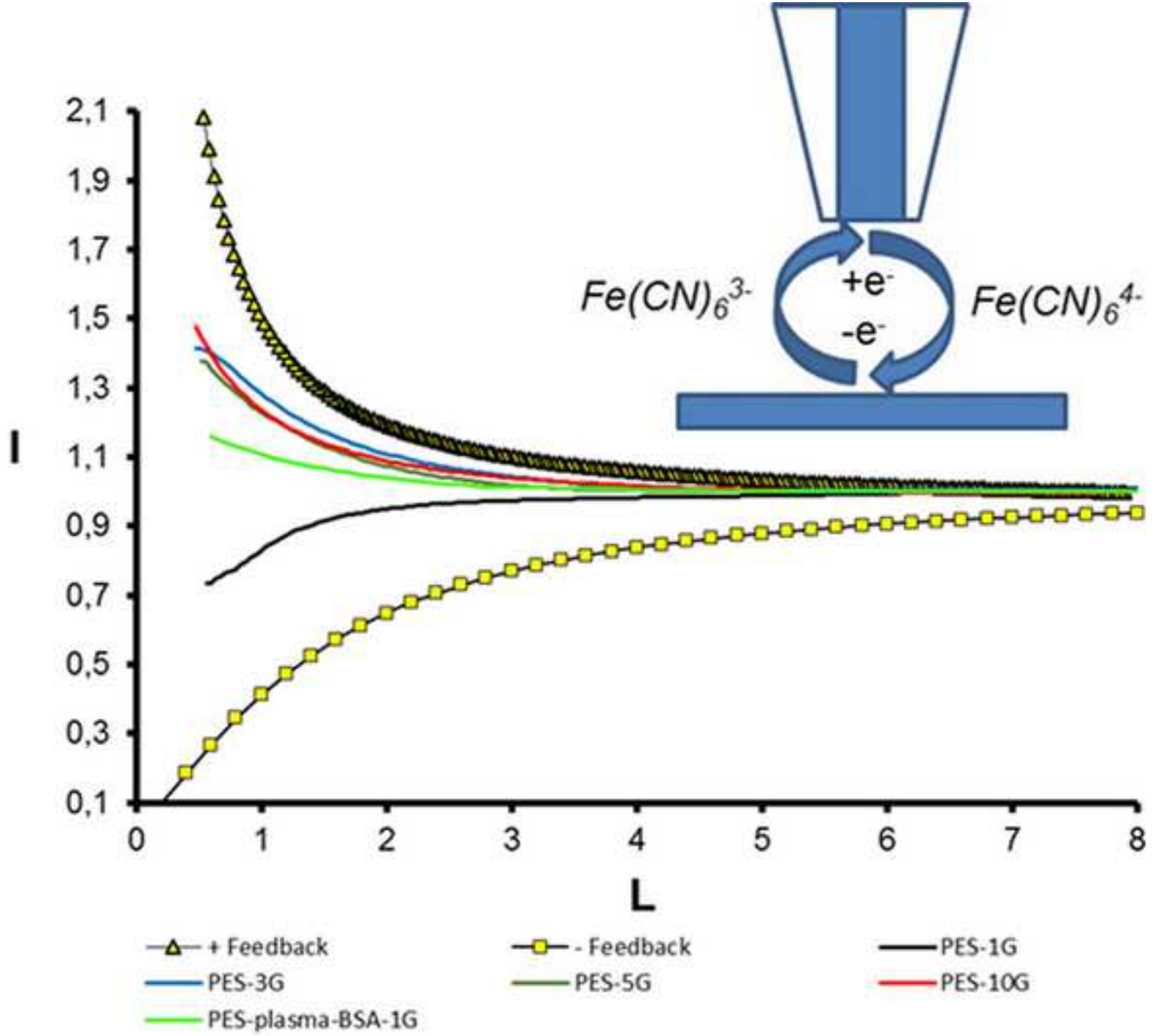

Figure 12

Click here to download high resolution image